AN ABSTRACT OF THE THESIS OF

Virendra S. Javadekar for the degree of Master of Science in Electrical and Computer Engineering presented on January 31, 1992.

Title : Design and Development of a Controller for a Brushless Doubly-Fed Automotive Alternator System

Abstract approved : _____
René Spée

The loads on the electrical systems of automobiles are projected to increase significantly in the near future. This will result in a requirement for improved efficiency over the present-day car alternators. An alternative scheme proposed at Oregon State University employs a Brushless Doubly-Fed Machine (BDFM) as an alternator.

This thesis begins with a study and characterization of the existing car alternator system. The configuration of the proposed scheme is discussed. In the proposed configuration, the power winding of the machine generates the bulk of the power and the control winding provides the excitation. The power winding feeds a power rectifier, which in turn charges the battery in an automobile. The control winding is supplied through an inverter. Issues related to inverter and rectifier design are discussed. A 3-phase pulse width

modulated inverter and a bridge rectifier were developed and tested for performance. A PSPICE simulation model for the rectifier was developed and results are compared with laboratory tests. A Voltage Regulator Circuit (VRC) and an Efficiency Maximizer Unit (EMU) for the system are designed and developed. A prototype alternator system is tested and the principle of efficiency maximization is verified. Finally, the comparative performance of the the existing and the proposed system is discussed and some recommendations for further improvements in the prototype system are made.

Design and Development of a Controller for a Brushless Doubly-Fed Automotive Alternator System

by

Virendra S. Javadekar

A THESIS

submitted to

Oregon State University

in partial fulfillment of
the requirements for the
degree of

Master of Science

Completed January 31, 1992

Commencement June 1992

APPROVED:

Redacted for Privacy

Assistant Professor of Electrical and Computer Engineering
in charge of major

Redacted for Privacy

Head of Department of Electrical and Computer Engineering

Redacted for Privacy

Dean of Graduate School

Date thesis is presented January 31, 1992

Typed by Virendra S. Javadekar

ACKNOWLEDGEMENTS

As I put together the outcome of the work of the past two years in this thesis, I realize that it would have been impossible for me to handle this task alone. I would like to take this opportunity to thank each and everyone who has helped me during this course.

First of all, I would like to express my sincere thanks to Dr. René Spée, who has been someone more than a Major Professor to me. I am grateful to him for his valuable guidance to me during my entire graduate program and thesis work. His trust in my abilities and enthusiasm for this project motivated me to work diligently.

I would also like to thank Dr. Alan K. Wallace and Dr. G. C. Alexander for their assistance to my thesis work and Dr. J. H. Herzog for helping me in completing the requirements of my graduate program. I am thankful to Prof. Amort who allowed me to use the equipment from the Instrumentation laboratory at various times during my thesis work. My thanks to Prof. Keith Levien for attending my defense in the capacity of a GCR.

The work described in this thesis was supported by a consortium consisting of The Bonneville Power Administration, Puget Sound Power and Light, and The Electric Power Research Institute. I am appreciative of the funding which made this work possible.

I acknowledge the assistance of my colleagues, D. K. Ravi, Ashok Ramchandran and Shibashis Bhowmik in conducting the laboratory tests.

At this moment, I cannot forget the strong moral support I have received from my family members in India for the last two years. I also thank Mr. Dhoot, Mr. Joshi and Mr. Vaidya for backing my decision of pursuing the M. S. degree.

Finally, I would like to dedicate this thesis to my Parents whose love and faith in me have always been my source of inspiration.

TABLE OF CONTENTS

LIST OF FIGURES

LIST OF TABLES

LIST OF APPENDIX FIGURES

Design and Development of a Controller for a Brushless Doubly-fed Automotive Alternator System

Chapter 1.

Introduction

Modern automobiles are equipped with electrical ancillaries that operate heaters, blowers, wipers, locks, power windows, etc. The concept of 'drive by wire' is being realized for improved performance of automobiles. Electrical devices and machines provide high efficiency, fast response, precise and easy electronic control, compact design and low maintenance and are therefore a logical choice for modern automotive systems. Because of increasing demand for more comfort and safety items, the loads on the electrical systems of automobiles are projected to increase up to 3 to 5 kW by the year 2000 [1] as against the present load of 1 to 2kW. This increase in power demand has forced radical changes in the electric power generation system of automobiles. The d.c. brush-type generator, which had been widely used till about year 1960, could not support the increased load due to commutation problems. The generators in use since then, in automotive electric power generation system (Fig. 1.1) are of the claw pole or Lundell construction, which is a readily-

manufactured (low-cost) and robust derivative of the conventional rotating d.c. field, synchronous generator.

The Lundell alternator uses a multiturn field coil embedded inside a claw-pole rotor to establish a multi-polar bidirectional field. The stator winding is a regular 3-phase winding feeding a diode bridge rectifier. The output voltage regulation is achieved by controlling the field winding current by means of a simple electronic feedback circuit.

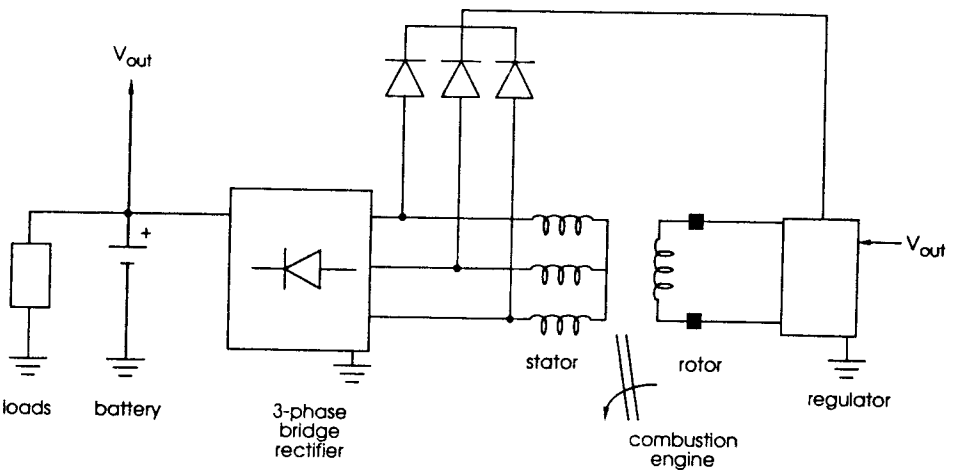

Fig. 1.1 Lundell Alternator System

However, the structure of this machine poses serious drawbacks; such as a complicated and inefficient magnetic circuit of predominantly solid steel and a high-windage rotor structure. This reduces the alternator efficiency as well as the output power capability for a given rotor diameter. The entire magnetic flux produced by the field coil has to pass axially through the magnetic core and the shaft. This construction causes the output power capability of the machine to be heavily dependent on the rotor diameter. The claw-pole structure

makes the solid (non-laminated) rotor structure imperative for manufacturing ease. However, this construction gives rise to eddy current losses in the rotor, which reduce the efficiency and increase the temperature of the field coil; thereby, further reducing the alternator output capability. Thus, machines with larger power output will be very bulky. This is impractical for future automobiles where compact and light accessories are needed to achieve a higher fuel efficiency.

A Lundell type alternator was completely characterized by subjecting it to load tests in the laboratory. The test set-up employed for this purpose is given in Fig. 1.2.

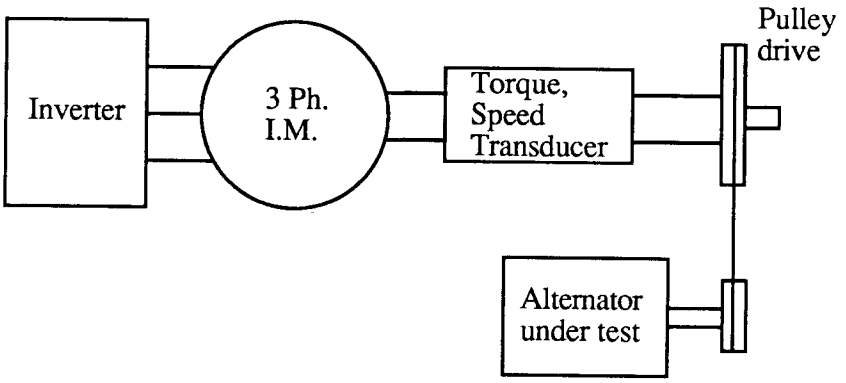

Fig. 1.2 Laboratory Test Set-up

The 3-phase induction motor serves as a prime mover and simulates the engine of an automobile. This motor is supplied by an inverter to achieve variable speed operation. The transducer mounted on the shaft provides torque and speed information. The alternator

under test is driven by a belt-pulley drive to step-up the speed (pulley ratio = 1.9) similar to that in an automobile.

A commercial Lundell-type alternator was acquired and tested for efficiency at various speed and load conditions. Sample test data and calculations are shown in Table 1.1.

Table 1.1 Sample Test Data for Lundell Alternator

Alt. speed (r/s)	Alt. torque (N-m)	Mech. power (W)	Output voltage (V)	Load current (A)	Alt. current (A)	Elect. power (W)	% Efficiency
85.8	1.2	659.6	14.3	15.7	17.7	253.1	38.4
93.0	1.2	687.4	14.3	15.7	17.7	253.1	36.8
100.1	1.2	725.3	14.3	15.7	17.6	251.7	34.7

where,

Mech. power = Total mechanical input power

= 2π [Alt. speed] [Alt. torque]

Alt. current = Total Alternator output current

= Load current + Battery charging current

Elect. power = Total electrical output power

= [Output voltage] [Alt. current]

% Efficiency = 100 [Elect. power / Mech. power]

The full load current rating of the alternator under test was 42A. In an automobile, the alternator operates over a speed range of 2000 to 6000 r/min i.e. 33 to 100 r/s. Also, it is required to maintain the output voltage at 14.5V.

Some important test results are shown here in the form of curves (Fig. 1.3).

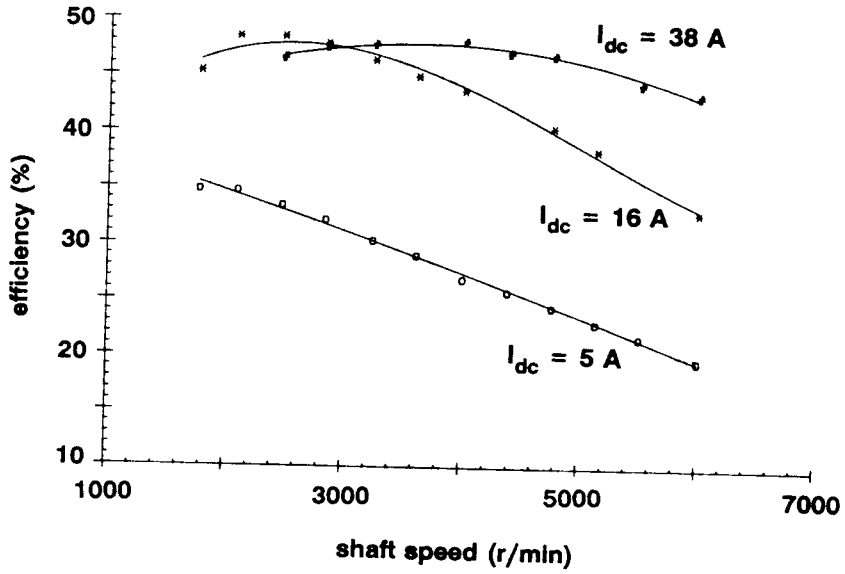

Fig. 1.3 Lundell Alternator Performance
(where I_{dc} = alternator current)

These results clearly indicate the poor efficiency of the present-day alternator. The performance of the system is worse at low speeds and loads as well as at very high speeds. The output voltage drops below 14.5V when the alternator is supplying high load current at low speed. This shows that the machine is optimized for a medium speed range at full load only and no provision is made to maintain the performance at other operating conditions.

The low efficiency of this present-day alternator has led to a re-examination of the automobile generator [1]. Highly-detailed, finite-element analyses are being applied to the improvement of the Lundell magnetic circuit [2]. The findings of the work are probably more appropriate to high per-unit cost aerospace generators than potential improvements to machines for automotive applications. It has been proposed that a reduction of the speed range, by use of a gearbox or adjustable pulleys, should be used to improve the Lundell generator efficiency [3]. However, these techniques, which are equally applicable to any variable speed generator, increase the system cost, reduce reliability and introduce some control difficulties. More fundamental improvements are possible if the Lundell generator is replaced by an inherently more efficient machine. For example, high efficiency induction machines are proposed as both the car engine starter (a low speed, high torque requirement) and the generator (a high speed variable torque system). However, the required power conditioning unit (PCU) has a very high rating and is expected to result in an expensive system in spite of being based on a robust, inexpensive machine.

Finally, recent advances in permanent magnet materials have resulted in high performance brushless d.c. motors which can be applied to car generator and starter systems [4]. Most likely, the permanent magnet a.c. generator will provide the best overall efficiency of any proposed system, because of zero excitation requirements. This must be traded off against potentially prohibitive capital costs caused by : (1) expensive magnet materials and construction cost; (2) large controllable power conversion unit and/or

gearbox required for voltage regulation. Problems have also been reported with the mechanical, thermal and corrosion properties of the advanced permanent magnet materials.

Another variable-speed generation system candidate has been proposed based on the brushless doubly-fed machine (BDFM) [5],[6]. The anticipated advantages are controllability (regulation) over wide operational ranges, competitive system cost based on inexpensive machine construction, low rating of the controller and uncontrolled (diode) power rectification. These features result in a robust, low maintenance configuration. A schematic of the proposed system is shown in Fig. 1.4.

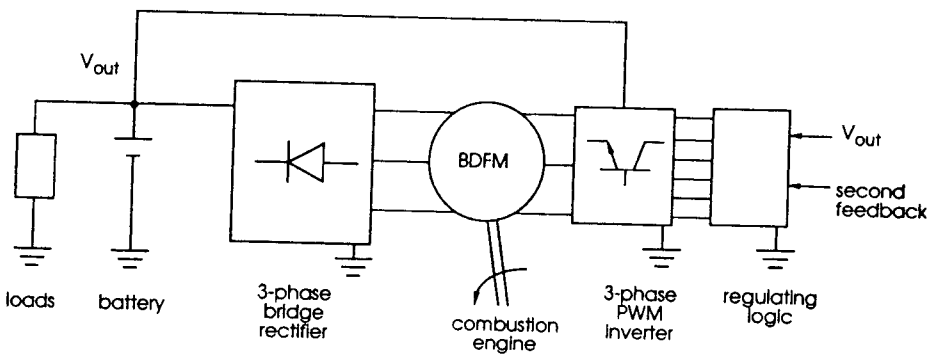

Fig. 1.4 Brushless Doubly-Fed Automotive Alternator System

The concept of the BDFM in itself is not new. It stems from the self-cascaded, or concatenated, induction machine [7],[8],[9]. When operated in conjunction with a controllable-current, controllable-sequence, bidirectional PCU, the self-cascaded machine is termed a brushless doubly-fed machine because of its connection-free rotor and two sets of three-phase stator windings. The BDFM has been shown to

enable variable-speed generation [10] or adjustable speed drives [11] with only a small percentage of the total power being processed by its PCU. Hence the PCU rating is small compared to that of the system, with the result that power electronic costs are significantly reduced. Moreover, the performance of the machine can be controlled by means of three control variables : control winding voltage magnitude, frequency and phase sequence. These features of controlled operational flexibility and potential competitive cost make the BDFM of interest for automotive applications. The BDFM is free from any size limitations both from the performance and manufacturing point of view and thus appears to be an appropriate alternative, especially for high power ratings (3 to 5 kW in case of an automobile alternator).

The goal of this thesis work was to design and develop a PCU and a controller for output voltage regulation and alternator efficiency maximization of the BDFM. Chapter 2 describes the design steps for the PCU, a 3-phase PWM inverter. The rectifier design follows in Chapter 3. The design of the voltage regulator and the efficiency maximizer is explained in Chapter 4. Results from the laboratory tests performed on the prototype alternator are presented in Chapter 5. Finally, conclusions and some recommendations for future improvements are presented in Chapter 6.

Chapter 2.

Design of a 3-Phase Pulse Width Modulated (PWM) Inverter

2.1 Selection of Inverter Topology

In the case of a BDFM system, the power conditioning unit (PCU) serves the purpose of supplying excitation to the control winding. The control winding is normally a balanced 3-phase, star-connected winding. In order to obtain maximum control over machine performance, a variable-voltage and variable-frequency excitation source is desirable.

In an automobile, the only source of electric power is the battery, which can provide d.c. power. While the control winding can be fed with d.c. power, this mode offers limited control and requires a chopper for excitation control. Therefore, an inverter (for d.c. to a.c. conversion) is required to interface the battery with the control winding.

There are many choices available with regard to the type of inverter such as a six-step or a square-wave switching inverter, a Pulse Width Modulated (PWM) switching inverter, a resonant inverter,etc.

In the case of a square-wave switching inverter, the output frequency can be varied by controlling the switching instants; but the output voltage has to be controlled by controlling the input d.c. link voltage to the inverter. The control circuit is simple, resulting in a low-cost configuration. Switching losses are low, but the inverter output contains a significant amount of low order harmonics.

The control circuit of a PWM inverter is more complex, but it allows adjustment of both the output voltage magnitude and frequency. Also, by keeping the switching frequency high compared to the desired output frequency, harmonics in the output can be pushed to higher frequencies where filtering is easier because of the inductive nature of the load. The disadvantage of this scheme is higher switching loss, which limits the switching frequency.

Resonant inverters are a relatively new class of inverters that provide for zero voltage and/or zero current switching of the power devices. This technique reduces the switching losses, thus enabling higher switching frequencies and device utilization. The drawback of these topologies is the requirement of a resonant circuit and complex control circuitry.

The proposed car alternator system requires a variable-voltage, variable-frequency inverter to act as an excitation source for the control winding. Also, since the efficiency is an important aspect, low harmonic content is desirable to avoid harmonic losses. Small size requirements mandate a compact power and control circuit with a low number of components. Therefore, the choice of a resonant converter is not justified, and a PWM inverter was chosen as a PCU. Of course, a six-step square wave output can also be obtained from the PWM inverter. Thus, the PWM inverter always allows the option of operating in the square wave switching mode.

2.2 Automotive PWM Inverter Design Considerations

PWM inverters are perhaps the most widely used type of inverter in industry. Nevertheless, the specific requirements of the BDFM alternator system necessitated the development of the inverter in-house rather than relying on an off-the-shelf design.

The application under consideration is a low-voltage, high-current application. The system voltage is normally 14.5V with some transient variations, which may result in voltage spikes up to 20V peak. The maximum current drawn by the control winding of the experimental machines was expected to be up to 20A rms at 9V (line) at approximately 0.5 p.f.

Normally, commercial inverters are designed for a high voltage (230/415 V) and a wide current range. Therefore, if a commercial inverter is to be selected for this application, it would be a mismatch with regard to the voltage rating.

In order to develop an inverter for the prototype car alternator, full understanding of the device usage is required. This can be achieved with the developed inverter; since it provides access to all the power devices for performance tests. Also, it is very easy to evaluate new power devices. Thus, optimum power device ratings for the prototype can be determined with the help of the breadboard inverter.

The control circuit for the PWM inverter provides for easy modifications of the relevant parameters like switching frequency, mode of operation (square wave or PWM), and base drive requirements. This allows greater flexibility of operation.

The control circuit of this inverter consists of the minimum number of components for a sinusoidal PWM inverter. It becomes evident that the entire circuit can be put on a single chip once the circuit parameters are determined after tests. Such devices, commercially known as 'smart power' devices, have been employed in the case of power supplies and drives.

Since the inverter was developed in the laboratory using relatively inexpensive components, it allows easy and low cost maintenance, troubleshooting and modifications.

2.3 Power Circuit Design : Selection of Devices and Topology

Various types of power devices are commercially available for switching applications like a PWM inverter.

Thyristors are inexpensive devices but impose a requirement of forced commutation. Gate Turn-Off thyristors (GTO's) are thyristor variants which can be turned-off by means of gate control. But the amount of power required to initiate this gate turn-off is quite considerable.

The Bipolar Junction Transistor (BJT) is a device that offers both controlled switching 'on' and 'off'. It is an inexpensive device and is simple to work with. It is a base-current-controlled device and is, therefore, relatively slow in switching operation. A BJT has very good conduction characteristics but comparatively poor switching characteristics.

The forward current gain (h_{fe}) of a BJT can be enhanced by connecting two or more devices in a Darlington configuration. This

increases the power handling capacity for the same base current, but reduces switching speed and also increases device losses.

Commercially, BJT's are available over a wide voltage and current range and therefore provide good selection for optimization.

The Metal Oxide Semiconductor Field Effect Transistor (MOSFET) is a voltage controlled device. This device is best suited for a high frequency application and offers very good switching characteristics. A positive temperature coefficient of resistance is an important feature of a MOSFET that provides some safety and easy paralleling. The drain-to-source resistance, $r_{ds(on)}$, is the parameter that determines the forward voltage drop across the MOSFET during conduction. Since this parameter is proportional to the die area it is low for high current devices, but can be considerable for low current MOSFETs.

An Insulated Gate Bipolar Transistor (IGBT) is a relatively new device. It is most suitable in the medium frequency range (20kHz-80kHz). Since it is a new device, it does not provide a wide range for selection and is available only in high voltage ratings. It also has an inherent problem of latch-up (a phenomenon when the gate loses turn-off control over the device) when it carries overcurrent.

This discussion indicates that a BJT or a MOSFET would be the right candidate for this application. The MOSFET has an upper edge over BJT so far as driving requirements are concerned. But more important issues are cost and forward voltage drop. MOSFETs with low current ratings would cause high voltage drop and those with high current ratings would be expensive as well as over-rated devices for this application. However, a very good selection of power BJT's is

available at the current and voltage ratings expected. These are less expensive and offer low forward voltage drop. Standard driver chips are available for base drive circuit design. Also, no external free-wheeling diodes across the collector-emitter are required; since these are integral in the transistor package.

The topology used for the inverter is the standard 3-leg topology with two devices in each leg. In order to simplify driving requirements, it is essential to use complementary devices in each leg. PNP transistors are used as top transistors and NPN transistors are used as bottom transistors as shown in Fig. 2.1.

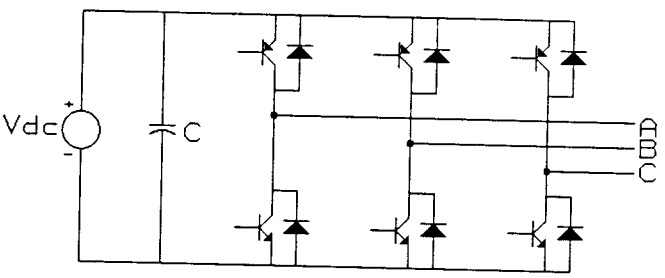

Fig. 2.1 Three Phase PWM Inverter

This arrangement eliminates the need of isolated power supplies for the top and bottom transistor base-drive circuitry. With complementary devices, when the base drive circuit of the top transistor (PNP) drives its base to ground, the transistor starts conducting and goes into saturation. When the base is connected to the d.c. link voltage the transistor turns 'off'. The base drive circuit has full control over the base current and the load voltage does not affect

the base current. The rating of the PNP transistor needs to be same as that of the bottom NPN transistor.

A prototype Brushless Doubly-Fed Automotive Alternator (BDFAA) was designed [6] for proof-of-concept-type tests. The machine has two isolated stator windings in the same stator frame. The power winding is wound for six poles and the control winding for two poles. The rotor has a nested loop structure. There are four nests with three loops in each nest forming a cage like rotor structure.

The maximum control winding current was estimated to be 20A (rms) using computer simulation data and applying reasonable limits. This calls for a device with approximately 28A ($\sqrt{2}$*20) current carrying capacity, which warrants the choice of a BJT with I_c = 30A. The system voltage is about 20Vdc maximum. Therefore the BJT should have a minimum of 20V forward blocking capacity. (i.e. V_{ceo} = 20V min.)

These two are the most important ratings which can be used for device selection. To satisfy these, Motorola MJ11011 PNP and MJ11012 NPN, Darlington power transistors were selected (refer to Appendix I for the data sheets). These devices have 30A collector current-carrying capacity and a voltage rating of 60V. This allows for some safety margin. Another device aspect to be examined is the Forward Bias Safe Operating Area (FBSOA). The FBSOA for switching or pulsed operation is normally larger than the FBSOA for d.c. operation (almost rectangular) because the device is capable of conducting heat during the 'off' period.

'On' voltages characteristics show that the collector-to-emitter voltage drop is low when the device is 'on'. This is a critical parameter

for automotive applications because the d.c. link voltage is regulated to 14.5 VDC. This mandates the use of low-voltage-drop devices to obtain maximum voltage output. The d.c. current gain of the device (the ratio of collector current to base current) is 500 (minimum) for 30A (maximum) collector current. This implies that a base current of 60mA minimum is required to keep the device in saturation over the entire current range. In practice, a higher value of base current is applied.

The devices have a built-in free-wheeling diode across the collector-emitter which is required as the load has an inductive nature. These diodes allow two-quadrant operation of the inverter i.e. the inverter can support forward motoring as well as regeneration. In other words, the active power flow can be from the battery to the control winding or vice versa if the control winding starts generating. This is an important feature which is utilized for efficiency maximization.

2.4 Inverter Control Circuit

The complete inverter control circuit can be grouped into three control units, which are functionally separate but are interdependent as shown in Fig. 2.2.

The control circuit that generates the actual PWM switching pattern is henceforth referred to as the Switching Pattern Generator (SPG). In order to maintain the output voltage at 14.5 VDC, a Voltage Regulator Circuit (VRC) is required. Moreover, to achieve the

maximum efficiency of operation, an Efficiency Maximizer Unit (EMU) unit is necessary.

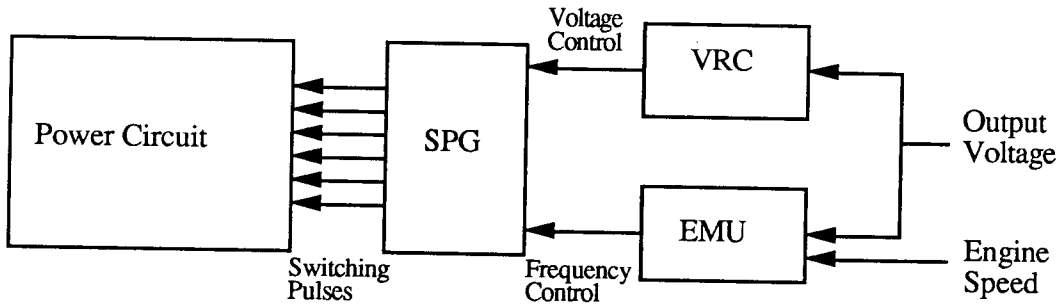

Fig. 2.2 Controller Block Diagram.

This section discusses the design and development of the SPG. The design of VRC and EMU follows in Chapter 4.

Numerous techniques are available to generate the switching pattern for a 3-phase PWM inverter. Sinusoidal PWM (SPWM) is perhaps the simplest method and is thoroughly discussed in the literature [12]. It can be easily implemented using analog components. The digital counterpart of this scheme involves asymmetrical or symmetrical sampling of the modulating wave [13]. With advancements in microprocessor technology, the use of microprocessors to generate switching patterns is also increasing [13]. Some other methods are selective harmonic elimination schemes [14], adaptive or hysteresis control [15], and space vector techniques [16].

However, for this application, the natural SPWM technique was selected because of its well-established, simple and very flexible nature. It can be implemented using a few low-cost components, while

still enabling good performance. The circuit, being mostly analog, can very well withstand the noisy environment (Electro-Magnetic Interference (EMI) from spark-plugs, solenoid switchings, etc.) in an automobile.

The technique employs a comparison of a high frequency triangular wave and a sine wave to obtain the switching instants as shown in Fig. 2.3 [12].

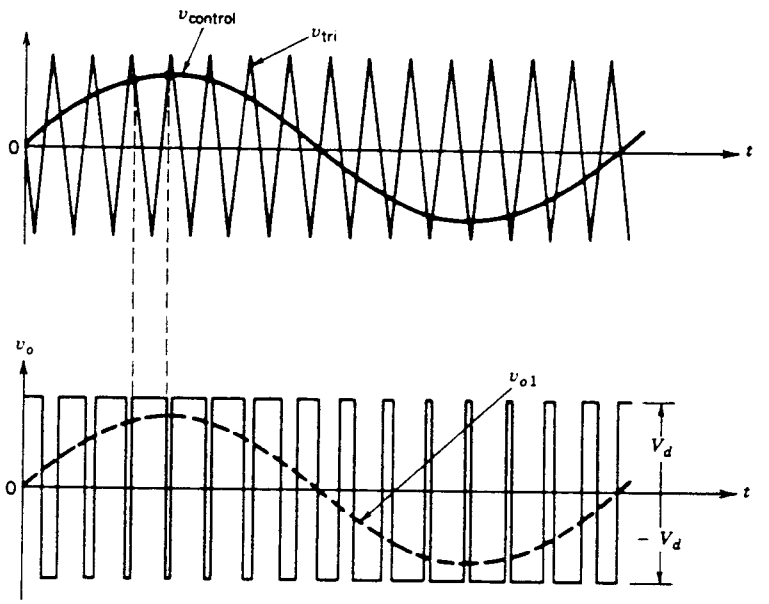

Fig. 2.3 Sinusoidal PWM Technique.

(From 'Power Electronics: Converters, Applications and Design' : Ned Mohan et al.)

where,

$v_{control}$: modulating voltage waveform

v_{tri} : carrier voltage waveform

v_o : instantaneous output voltage waveform

V_{o1} : output voltage fundamental component

V_d : d.c. link voltage

The triangular wave, also referred to as the carrier wave, decides the switching frequency. The output voltage magnitude and frequency depends upon the amplitude and the frequency of the sine wave or the modulating wave. In case of a 3-phase PWM inverter, only one carrier wave is sufficient but three sine waves displaced by 120^o are required as modulating waveforms.

The ratio of the modulating wave amplitude to the carrier wave amplitude is known as Amplitude Modulation Ratio (M_a). The ratio of the carrier wave frequency to the modulating wave frequency is known as Frequency Modulation Ratio (M_f). Fig. 2.4 [12] shows the inverter output line voltage harmonic spectrum for a high M_f. Fig. 2.5 [12] shows the ratio of inverter output line voltage to the d.c. link voltage as a function of M_a (for an ideal case).

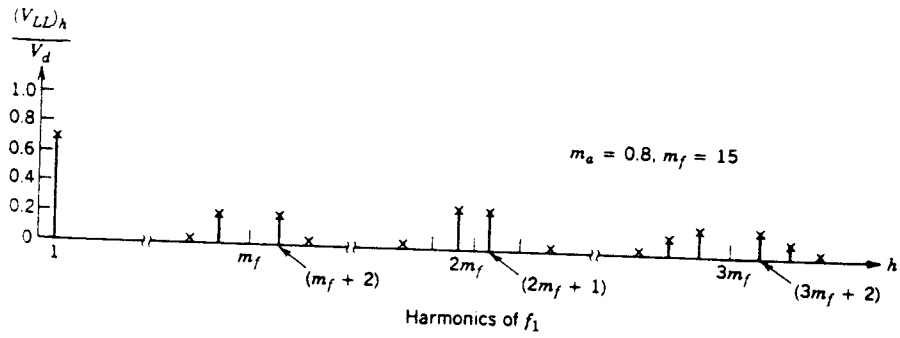

Fig. 2.4 Output Voltage Harmonic Spectrum

(From 'Power Electronics: Converters, Applications and Design' : Ned Mohan et al.)

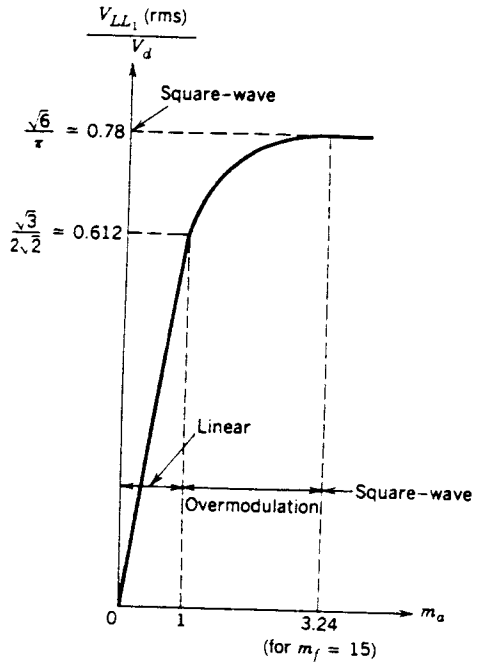

Fig. 2.5 Output Voltage Vs. M_a

(From 'Power Electronics: Converters, Applications and Design' : Ned Mohan et al.)

A hybrid (digital and analog) circuit [17] is developed to generate these waveforms, which are used to obtain the PWM switching pattern. Fig. 2.6 shows the scheme in a block-diagram form. For detailed circuit diagram refer to Appendix II.

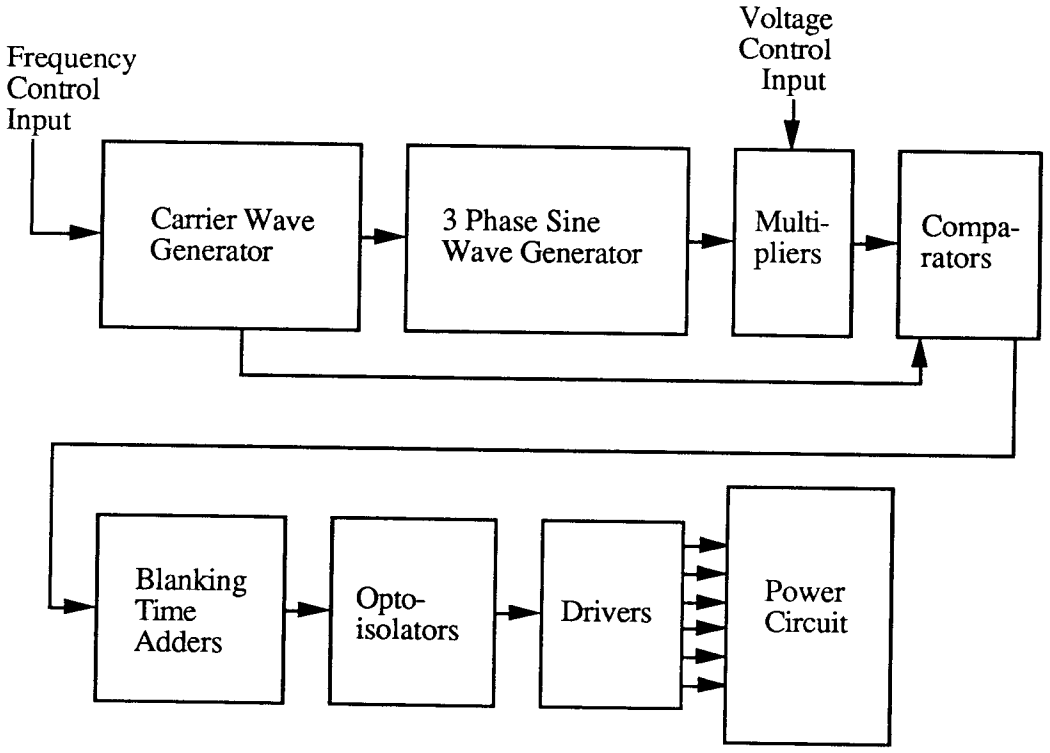

Fig. 2.6 PWM Pattern Generator (SPG).

A Digitally Controlled Analog Switch (DCAS), an integrator and a Schmitt trigger form a closed loop circuit to generate a triangular carrier wave and a square wave, the frequency of which depends upon a voltage reference input signal. The square wave is then passed through a frequency divider and flip-flops to generate a low frequency 3-phase square wave. In turn, the square waves are used to generate three triangular waves of constant amplitude. Three 'FET sine-shaper' circuits then shape these triangular waves into sine waves, which are subsequently multiplied by the amplitude reference voltage signal.

Thus, the triangular carrier wave and the three sinusoidal modulating waves are now available. Fig. 2.7 shows a plot of these waveforms obtained in the laboratory.

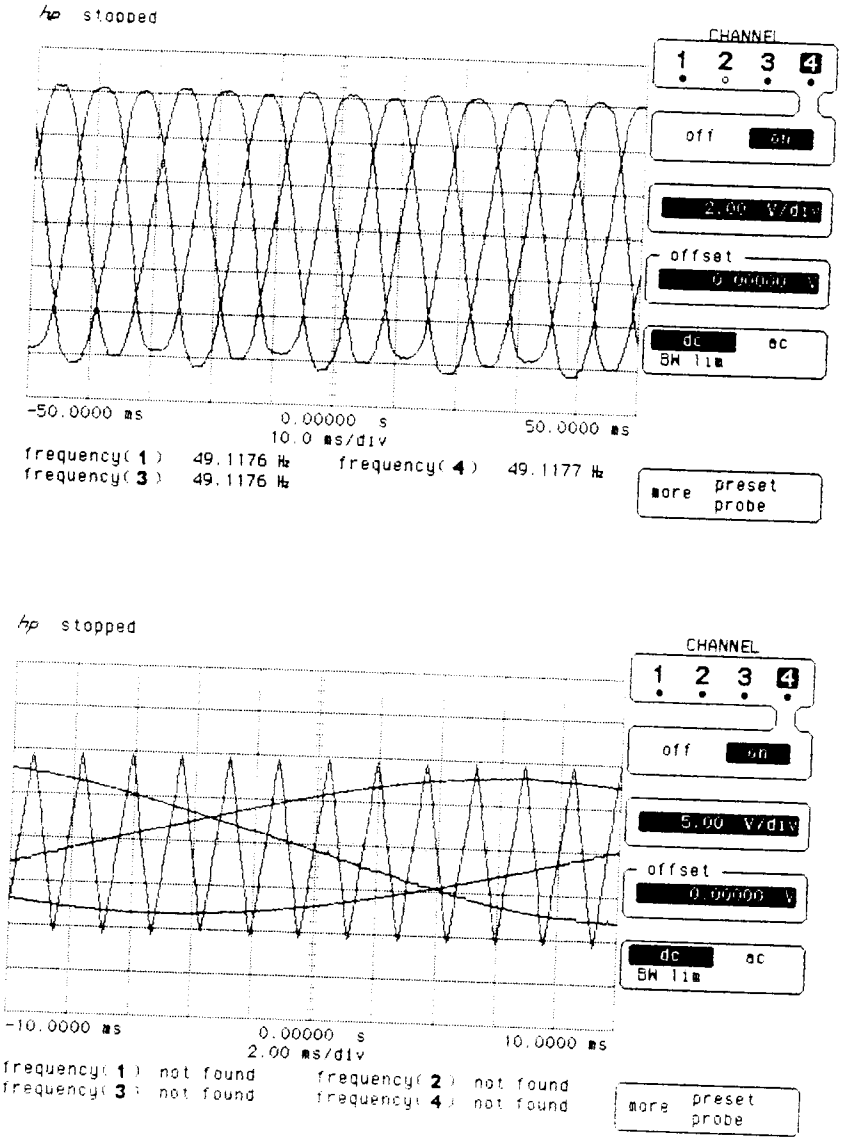

Fig. 2.7 Modulating and Carrier Waveforms

(vertical scale : 2V/div for top plot and 5v/div for bottom plot)

Operational-amplifier (Op-amp) comparators are employed to generate the switching pattern through a comparison of the carrier wave and each of the three modulating waves. The pulses obtained are

then passed through a blanking-time addition circuit, which is nothing but a polarized RC network. The blanking time prevents the occurrence of any shoot-through fault. The RC circuit is followed by a Schmitt trigger which is required to restore the rectangular shape of the pulses. These pulses are then fed to the opto-isolators, whose outputs are connected to the driver chip. The driver chip outputs drive the base terminals of the bottom (NPN) transistors directly. However, the base terminals of the top (PNP) transistors are driven through base drive transistors, in order to perform the necessary inversion.

2.5 Inverter Performance

The performance of the inverter is determined by testing it for efficiency and output harmonic spectra.

Assuming ideal switches as well as ideal circuit conditions and sinusoidal output waveforms, the input-output equation for an inverter can be written as:

$$[V_{dc}]\,[I_{dc}] = \sqrt{3}\;[V_{ll}]\,[\,I_{ll}]\,[\,\cos\phi\,] \qquad (2.5\text{-}1)$$

where,

V_{dc} : D.C. link voltage.

I_{dc} : D.C. link current.

V_{ll} : Inverter output voltage (line-to-line).

I_{ll} : Inverter output current (line-to-line).

$\cos\phi$: load power factor.

In a practical situation, the switches are not ideal, but have switching and conduction power loss associated with them. Also, the

harmonics in the output voltage and current waveform reduce the useful output power, as only the fundamental of the voltage and current convey the useful power. The inverter control circuit and the base-drive circuit for the power transistors also consume some power. All these factors bring down the inverter efficiency.

Tests were carried out on the prototype inverter to determine its efficiency at various load and frequency conditions. An R-L (resistive and inductive) combination is the most commonly encountered load type. A highly inductive load attenuates the high frequency current harmonics and, thus, reduces harmonic losses. However, due to unavailability of suitable inductors (1-5 mH), very low value inductors (250 μH) along with rheostats were used to form a three phase star connected load.

The test results are given in Table 2.1.

Table 2.1 Inverter Test Data

Frequ -ency (Hz)	Switch-ing freq. (Hz)	Output line Voltage (V) rms	Output Current (A) rms	Load P.F.	Output Power (W)	D.C. Link Voltage (V)	D.C. Link Current (A)	Input Power (W)	%Effi-ciency
80	2880	7.5	9.5	0.92	113.6	14.5	16	232	49.0
80	2880	5.3	6.7	0.92	56.5	14.5	8	116	48.7
80	2880	3.4	3.6	0.92	19.0	14.5	4	58	32.8
40	1440	7.2	9.5	0.98	115.9	14.5	17	261	47.1
40	1440	4.4	5.9	0.98	44.0	14.5	8	116	38.0
40	1440	2.7	3.2	0.98	14.7	14.5	4	58	25.4

Curves of efficiency Vs. output power is shown in Fig. 2.8.

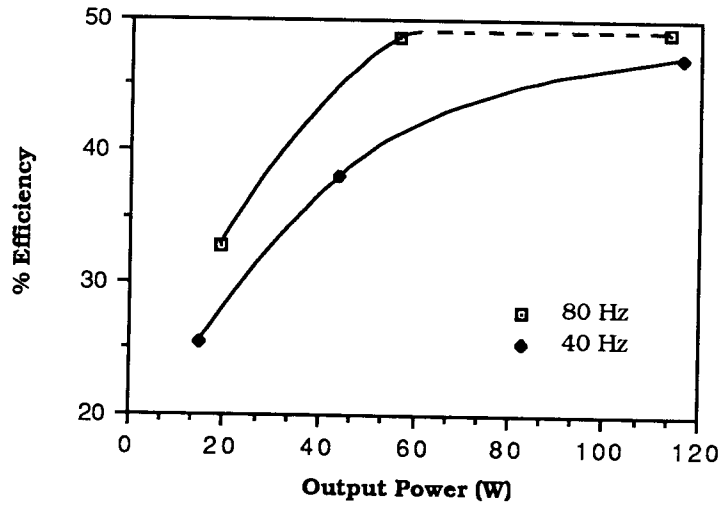

Fig. 2.8 Inverter Performance

(for output frequency = 80 Hz, switching frequency = 2880 Hz)

(for output frequency = 40 Hz, switching frequency = 1440 Hz)

The rated output of the inverter is around 125VA. The curves indicate that the efficiency is about 50% near rated output and it drops at lower output levels. The main reason for this is the device switching and conduction losses. Near rated output power, the device loss accounts for about 35% of the input power, the remaining 15% can be attributed to harmonic and control circuit losses. However, as the output power is reduced, the device loss becomes a significant percentage and thus brings down the efficiency even further. The efficiency is better at 80Hz operation because of lower harmonic losses at higher frequency.

Figs. 2.9 (a), (b), (c) show the harmonic spectra of the output voltage. It is clear that PWM operation pushes the harmonics to higher

frequencies. The square-wave-mode of operation introduces a significant amount of lower order harmonic but, at the same time, provides a higher fundamental voltage component. Fig. 2.10 is a sample output current waveform when the inverter is operated in the PWM mode.

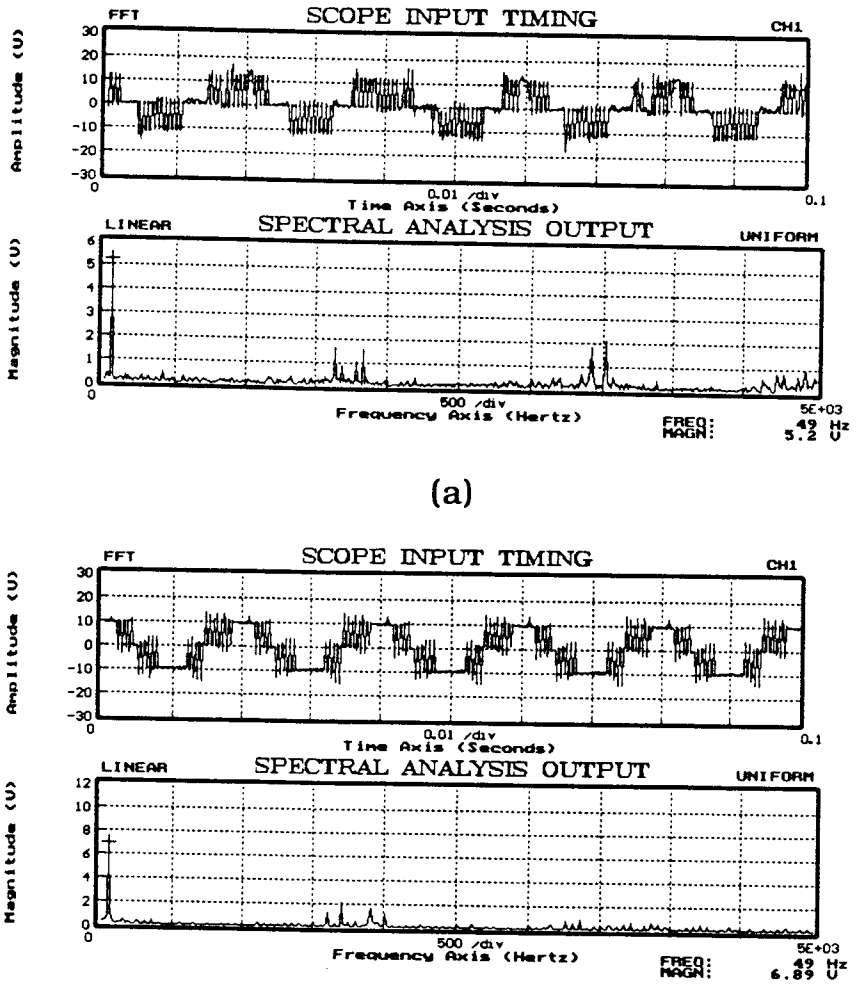

Fig. 2.9 Inverter Output Voltage Spectra

(a) PWM Operation

(b) PWM Operation with Pulse Dropping

(c) Square Wave Operation

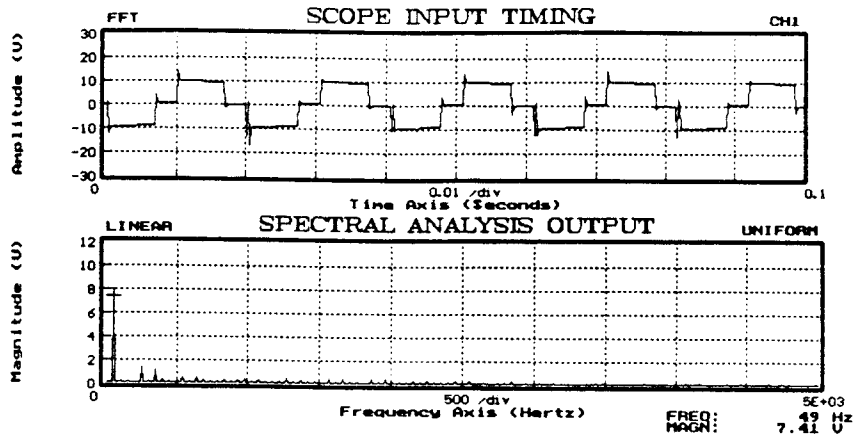

(c)

Fig. 2.9 Inverter Output Voltage Spectra (Continued)

(a) PWM Operation

(b) PWM Operation with Pulse Dropping

(c) Square Wave Operation

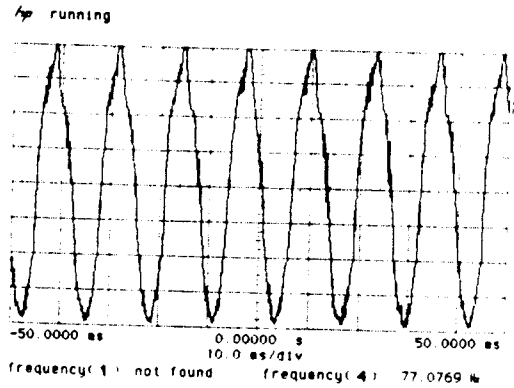

Fig. 2.10 Inverter Output Current Waveform

(vertical scale : 5V/div)

Chapter 3.

Design of 3-Phase Power Rectifier

3.1 Device Selection and Design

The output from the alternator power winding is a.c. and needs rectification before it can be used to charge the battery and supply loads. A three-phase diode rectifier in bridge configuration as shown in Fig. 3.1 is designed for this purpose. This rectifier is also present in the Lundell alternator for the same purpose.

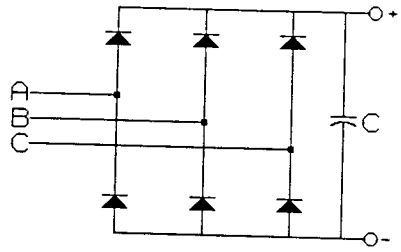

Fig. 3.1 Three-Phase Bridge Rectifier

The full-load current is assumed to be 42A (equivalent to the commercial Lundell alternator under test). Also, the rectifier needs to provide for the copper losses in the control winding. The magnetizing current flowing in the control winding is purely reactive and appears as ripple on the inverter d.c. link current. The rectifier has to carry this peak ripple current. Therefore, its rating needs to be increased.

The rectifier is a six-pulse rectifier. Therefore, each diode conducts for only 120^{o} in a cycle. If the rectifier is assumed to supply full load current (42A) in a continuous manner, then the average

forward current flowing through each diode is 14A. The rectifier is also required to provide for the d.c. link input current to the inverter. This current is estimated to be a maximum a 25A (i.e. average 8A per diode). Therefore, 40A devices are selected, allowing reasonable safety margin. The reverse voltage rating of the device is the a.c. peak value of the alternator output voltage (line-to-line). Under dynamic load conditions, when a large load is switched off, the alternator output voltage may shoot up because of the delay imposed by the response time of the regulator circuit. The worst case would be switching from full load to no load. To test the system, a bridge rectifier was built using 1N1184A diodes (refer to Appendix I for data sheets). These are ordinary power diodes for general rectifier application. The system was tested using this rectifier. The voltage spike is measured to be about 20V (peak) experimentally, which is well within the 100V rating of these diodes.

However, for best performance, it is imperative to use low forward voltage drop diodes for the rectifier. This reduces the rectifier losses and also improves the output voltage and overall efficiency. To achieve this, Schottky barrier diodes Motorola 1N5834 were employed. These are 40A, 40V devices and are optimum for this application (refer to Appendix I for data sheets).

3.2 PSPICE Simulation and Laboratory Performance Tests

The three phase bridge rectifier is a critical part in the car alternator system since it has to carry all the load current and the d.c. link current for the inverter. It needs to be highly efficient to ensure a high overall system efficiency.

A PSPICE simulation program is set up to test the performance of the rectifier. Fig 3.2 shows the simulated circuit. The alternator is simulated using sinusoidal voltage sources. The fundamental output frequency of the alternator (6-pole side) is selected as 320Hz (synchronous operation; 80Hz 2-pole excitation frequency; 6000 r/min rotor speed; negative sequence operation). In order to better represent the winding distribution [18], a third harmonic component (1/3 amplitude and negative phase sequence with respect to the fundamental) is also modelled using series voltage sources. The stator impedance consisting of phase resistance and inductance is connected in each phase. A three phase bridge rectifier is set up using 1N5834 diodes from the PSPICE device library. A filter capacitor (5000 μF) is connected across the rectifier output.

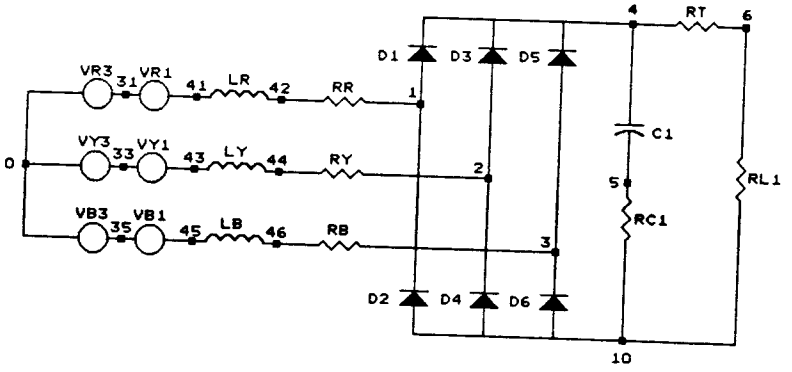

Fig. 3.2 PSPICE Simulation Model

For efficiency considerations, it is important to take into account lead resistance of the cable from the rectifier to the battery or load. A 10 AWG wire size was assumed. A 5mΩ resistance corresponding to 5

feet of cable was added to the circuit. The stator-side cable resistance was neglected; since the rectifier is placed very close to the stator winding during normal operation.

The rectifier was tested for 20A and 40A load currents. The load was simulated using a resistor.

To compare the simulation results and actual performance, the simulation program is also run with 60Hz voltage sources feeding the rectifier. The rectifier is tested in the laboratory for 60Hz operation, with a three phase autotransformer feeding the a.c. side of the rectifier. The filtered output is connected to rheostats forming the load. The simulation results and the test results for 60Hz as well as 320Hz operation are summarized in Table 3.1.

Table 3.1 Rectifier Test Data

			Simulation Results		Test Results			
Freq-ency (Hz)	Load Current (A)	Load Voltage (V)	Input Power (W)	% Effici-ency	Input line Voltage (V) rms	Input Current (A) rms	Power Factor	% Effici-ency
60	20	14.5	300	96.7	12.4	15.0	0.94	96.0
60	40	14.5	638	90.9	13.6	29.0	0.95	89.5
320	20	14.5	305	95.1	12.8	14.6	0.94	95.4
320	40	14.5	642	90.3	N/A	N/A	N/A	N/A

where,

% Efficiency = 100 [Output Power / Input Power]

Output Power = [Load Voltage] [Load Current]

Input Power = $\sqrt{3}$ [Input Voltage] [Input Current] [Power Factor]

In order to calculate the rectifier efficiency, only input power and output power are required. With PSPICE, it is convenient to compute the input power by adding the instantaneous power waveforms of the three phases and then taking the average of the resultant waveform rather than determining the input power using the current and voltage true RMS values which are not easily available. For laboratory tests, a power profiler was used which provides the power as well as true RMS voltage and current values with power factor. These figures are included in the table to give a better idea of the magnitudes of voltage and current involved.

A simulation plot for the diode forward voltage drop for 40A load current is shown in fig. 3.3. Actual diode forward voltage drop for 40A load current is shown in Fig. 3.4, a plot obtained during the laboratory tests.

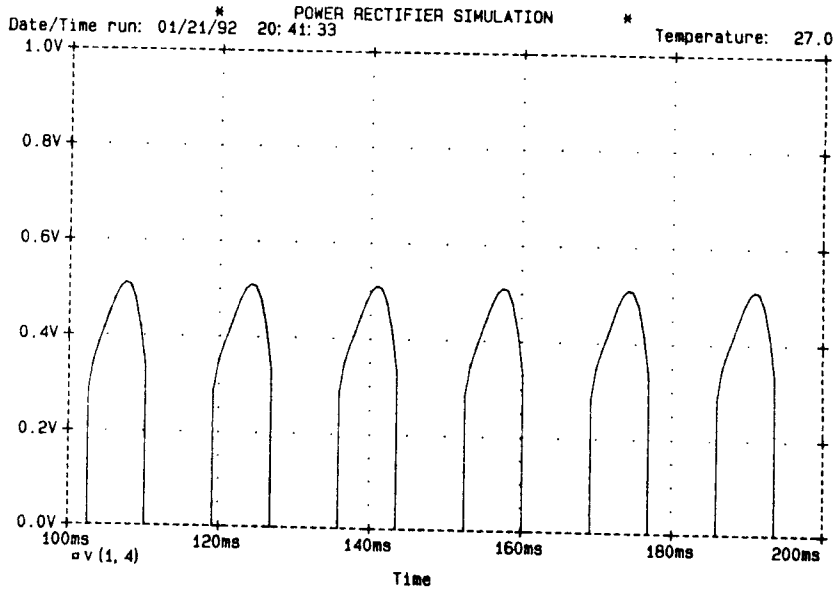

Fig 3.3 Diode Forward Voltage Drop (Simulation)

(60Hz Operation)

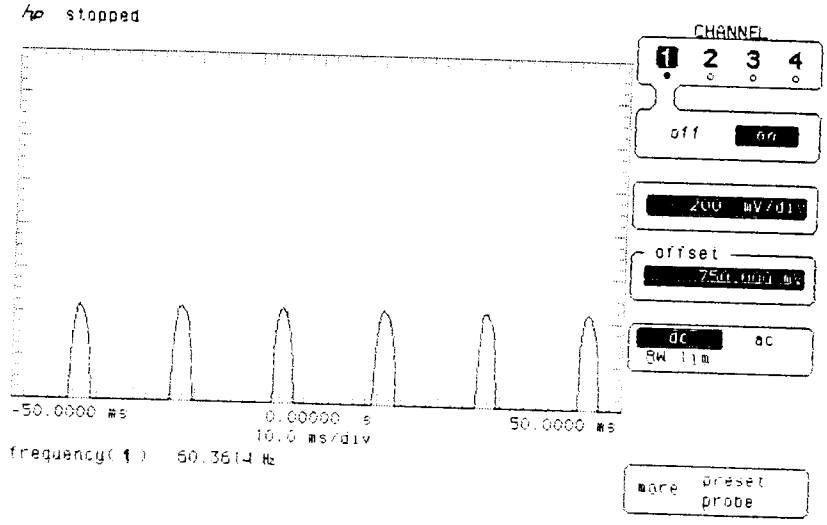

Fig 3.4 Diode Voltage Drop (Laboratory Test)

(vertical scale : 200mV/div)

(60Hz Operation)

The simulation results and the test results closely match. The rectifier efficiency is quite high aiding the efficient operation of the alternator system. However, it should be noted that the simulation is carried out at 27^{o}C; rectifier losses will increase for operation at higher temperature, thus decreasing the efficiency. The model can be used to predict the performance at higher temperatures by using the '.TEMP' command.

Chapter 4
Design of Voltage Regulator and Efficiency Maximizer

4.1 Design of the Voltage Regulator

A recommended practice [19] is that the car alternator should be capable of maintaining 14.5V while delivering the full-load current (i.e. 42A in the case of the tested commercial alternator). As in the case of any alternator, in the absence of a regulator, the output voltage would drop with increase in load current. The main reason for this is the voltage drop in the winding itself. Therefore, it becomes necessary to boost the generated internal e.m.f. to compensate for this drop. This can be achieved by increasing the excitation or the field current, assuming a constant speed of operation.

In the case of the BDFAA, the excitation can be controlled through the inverter feeding the control winding. The d.c. link of the inverter is the d.c. bus across which the battery and the other loads are connected. The inverter output voltage and frequency both determine the control winding current. If the frequency is assumed to be constant, the excitation depends solely on the inverter output voltage. For simplicity, the following discussion assumes a constant inverter output frequency. It is also assumed that the d.c. link voltage stays constant at 14.5V and the machine can support full load current at the assumed excitation frequency; i.e. the impedance of the control winding is such that enough excitation current can be supplied with the inverter output line voltage limited to about 9V. The implications of these assumptions are explained later in this section.

The control strategy employed to regulate the inverter output voltage and hence, the alternator output voltage, is standard output feedback control. Fig. 4.1 shows the Voltage Regulator Circuit (VRC) scheme in block diagram form. A detailed circuit diagram can be found in Appendix II.

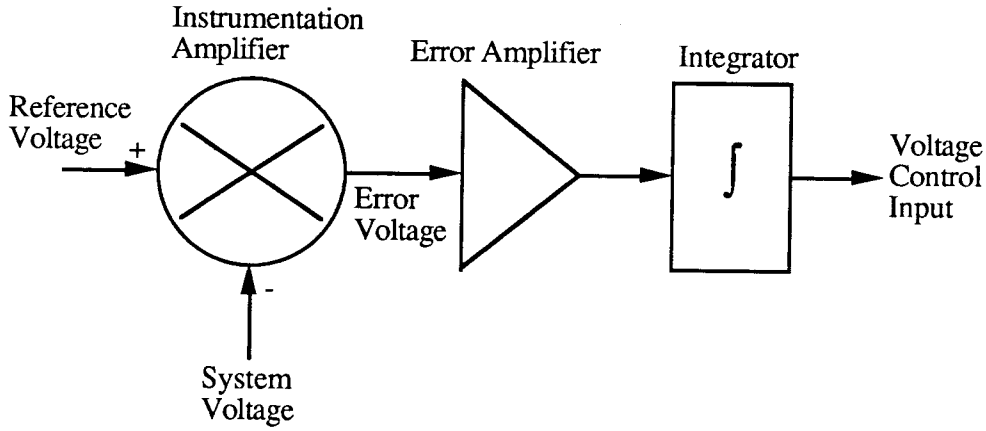

Fig. 4.1 Voltage Regulator

(The 'Voltage Control Input' goes to SPG (Fig. 2.6))

A reference corresponding to 14.5V is set up using an auxiliary power supply. In a practical automotive application, this may not be possible and a reference voltage using a zener diode may have to be generated. The system voltage is also properly scaled using a potential divider. The calibration procedure simply involves adjusting the potential divider such that the error between the reference voltage and the scaled system voltage is reduced to zero when the system voltage is 14.5V. An error amplifier circuit is used to amplify any error that occurs during normal operation. The error signal is then fed to a

Proportional-Integral (PI) controller. An op-amp integrator [20] performs the necessary integration. The output of the PI controller is connected to the multiplier circuits in the SPG. Thus, the output of the PI controller controls the amplitude of the three reference sine waves and hence the inverter output voltage.

A pure proportional control causes severe output voltage oscillations under load conditions. Therefore, PI control is required. A step increase in load current causes a dip in system voltage, resulting in a step change in the error amplifier output, i.e. the PI controller input. The PI controller then ramps up the inverter output voltage and brings the system voltage back to 14.5V. When the error reduces to zero, the output of the PI controller stays constant, thus maintaining the output voltage and current. As the battery is being charged, the voltage tends to rise above 14.5V, causing negative error. This slowly brings down the PI controller output until the voltage remains steady at 14.5V. These oscillations are very small (within 0.1V), and finally the system settles to 14.5V with constant inverter output.

A step reduction in load current causes a momentary rise in the system voltage, producing a large negative error at the PI controller input. This would cause the PI controller output to swing negative. However, multiplier circuits perform multiplication of the input modulus only. Therefore, a diode is connected at the PI controller output to block the negative input to the multipliers. In such a case, a zero input to the multipliers brings down inverter output to a minimum. This reduces the system voltage back to 14.5V.

The integral control reduces the steady state error to zero and it can easily be adjusted to obtain very low overshoots. But the response

is slightly sluggish. The gains need to be adjusted such that the response is fast enough for large load changes. This is especially true for a sudden load increase. If the response is not fast enough, the battery starts discharging and the system voltage can drop to a very low value (less than 10V). This results in a reduced d.c. link input voltage to the inverter, causing reduced inverter output voltage. With reduced excitation, the system voltage drops further and system output decays beyond recovery. However, this behavior is the result of the initial assumption of constant speed and frequency.

One possible way to avoid this system crash is to increase the speed of rotation to enhance generation at the same excitation level. But this is not practical; since the engine speed would be decided by the driver and cannot be changed to meet the alternator requirements.

System voltage response to step increases in load can also be controlled by reducing the inverter output frequency. This reduces the impedance of the control winding, allowing more excitation current to flow for a given inverter output voltage. Increased excitation in turn increases the output voltage and the system can recover. This action is taken by the EMU and is explained in more detail in Section 4.3.

4.2 Performance Tests on VRC

The dynamic performance of the VRC is tested by subjecting the prototype alternator system to a step change in load current from no load to 25A. Standard control system parameters [21] are measured from the response obtained. Fig. 4.2 shows the plot of the system

voltage (trace A) and the regulator output voltage(trace B). The glitches in the waveforms are because of the pick-up during measurements.

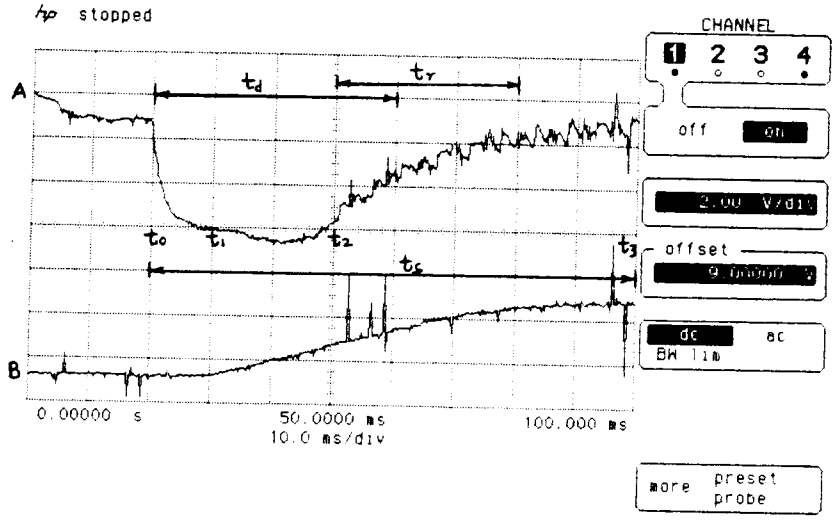

Fig. 4.2 VRC Performance

(Trace A : system voltage waveform)

(Trace B : regulator output voltage waveform)

(vertical scale : 2V/division)

The system voltage is seen to drop for some time after the application of load at t_0. Then the regulator starts correcting the error at time t_1. However, because of a delay caused by the SPG and various inductances, the output voltage continues to drop for some more time, until t_2, and reaches a low of approximately 9V . Thereafter, because of the increased inverter output, the output voltage starts recovering and comes back to 14.5V at t_3.

The 'delay time (t_d)' of the system, defined as the time required for the step response to reach 50% of its final value, is 40ms. The 'rise

time (t_r)', defined as the time required for the step response to rise from 10% to 90% of its final value, is 30ms. The 'settling time (t_s)' of the system, defined as the time required for the step response to stay within a specified percentage (5%, in case of an automotive alternator) of its final value, is 80ms. For an automotive application this recovery is fast enough. Also, it can be seen that there is no overshoot, indicating that the system is well-damped.

The performance of the prototype system is found to be satisfactory for all load changes up to a maximum of 25A with the alternator running at 6000 rev/min. At lower speeds the maximum output current capability of the alternator reduces. If a load higher than 25A is applied the system voltage drops and stays at some value lower than 14.5V.

4.3 Efficiency Maximizer Unit (EMU)

The conventional Lundell alternator has no provision for improving the efficiency at any operating point, since the only control variable, the field current, is used for output voltage control. However, in the case of a BDFAA, two control variables are available. As discussed in Section 4.1, the inverter output voltage is utilized to control the system voltage. This leaves the other variable, i.e. the inverter output frequency, free for efficiency improvement. The inverter output frequency can be controlled by controlling the voltage level at the 'Frequency Control Input' of the SPG (Fig. 2.6). The phase sequence of the inverter output can also be controlled.

In order to understand the efficiency maximization principle, it is necessary to examine the field relationships in a BDFM. Fig. 4.3 shows the relative directions and velocities of the fields existing in a BDFM.

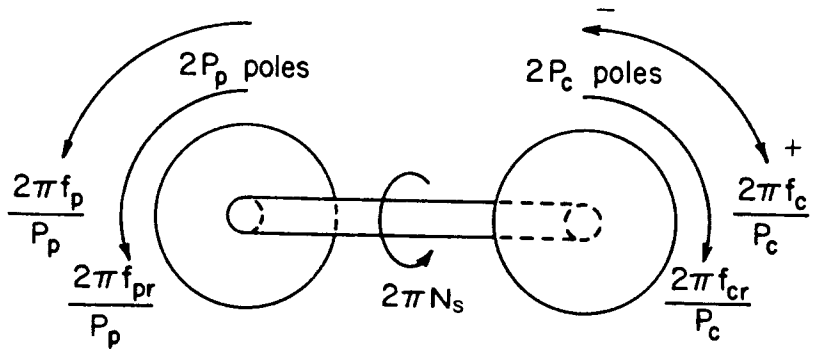

Fig. 4.3 Field Relationships

where,

f_p : power winding frequency

P_p : number of power winding pole pairs

f_{pr} : power winding induced rotor frequency

N_s : rotor angular velocity (rev/s)

f_c : control winding frequency

f_{cr} : control winding induced rotor frequency

P_c : number of control winding pole pairs

and for synchronous operation $f_{pr} = f_{cr}$.

For normal generator operation, the power winding field rotates in the same direction as the rotor. However, the control winding excitation phase sequence can be adjusted; therefore, the control winding field can rotate in either direction. The phase sequence which causes the control winding field to rotate in the opposite

direction of the power winding field is referred to as 'Positive Sequence'; co-rotational fields are obtained with 'Negative Sequence' excitation. Thus, in 'Negative Sequence Operation', power winding and control winding fields rotate in the same direction as the rotor.

The control winding behavior is similar to an induction machine. It should be noted here that as the power winding feeds a rectifier, it operates at a near unity displacement power factor. Thus, all the excitation, i.e. the reactive magnetizing power for the machine, must be provided by the inverter supplying the control winding. It should also be noted that mechanical rotor speed is determined by the engine speed and hence is not a controllable variable.

In 'Positive Sequence Operation', the active power flow is always into the control winding, irrespective of the excitation frequency and the rotor speed. Since the control winding field always rotates in a direction opposite to the rotor rotation, the operation is equivalent to 'plugging'. The slip is always positive and greater than 1, resulting in lossy operation.

However, in 'Negative Sequence Operation', the active power flow can be into or out of the control winding, depending upon the excitation frequency and the rotor speed. If the excitation frequency is less than the rotor speed (assuming a 2-pole control winding), 'induction generator action' (negative slip) takes place and the control winding starts generating active power while continuing to draw the required reactive power. Since the control winding is supplied by a bidirectional inverter, active power can flow back to the d.c. link. But the d.c. link voltage (battery voltage) is fixed at 14.5V and therefore the generated voltage must be high enough to allow the inverter

diodes to conduct. Whether the control winding would be able to charge the battery or not depends on various factors like machine parameters, the load on the battery, excitation frequency and voltage, rotor speed, etc. But it is clear that the 'Negative Sequence Operation' of the prototype alternator promises a way to improve the overall system efficiency by means of power generation using both windings. However, the desired 'induction generator' action imposes an upper limit on the control winding excitation frequency. An engine speed feedback is thus desirable to minimize the search time for the best efficiency point.

Also, in order to keep the copper losses in the control winding to a minimum, the excitation current should be reduced to a minimum. This can be achieved by increasing the excitation frequency. The frequency can be increased so long as enough voltage is available at the inverter output to supply the minimum required excitation. Once the maximum inverter output voltage is reached (limited by the d.c. link), any increase in frequency will result in a reduction of excitation current below the required minimum. In turn, this will cause a reduction of alternator output voltage.

Thus, it can be seen that in the case of the prototype alternator, the EMU needs to be sensitive to rotor speed variations caused by engine speed changes and system voltage variations because of load changes. Using a 'Negative Sequence Operation', the EMU has to generate a 'Frequency Control Input' for the SPG. This signal should be such that the excitation frequency causes the maximum possible active power flow out of the control winding, corresponding to the operating point. However, under some load and speed conditions, it may not be

possible to achieve power flow out of control winding. Under these circumstances, the EMU should lower the excitation frequency just enough to maintain the alternator output voltage.

A flow-chart describing the EMU operation is shown in Fig. 4.4.

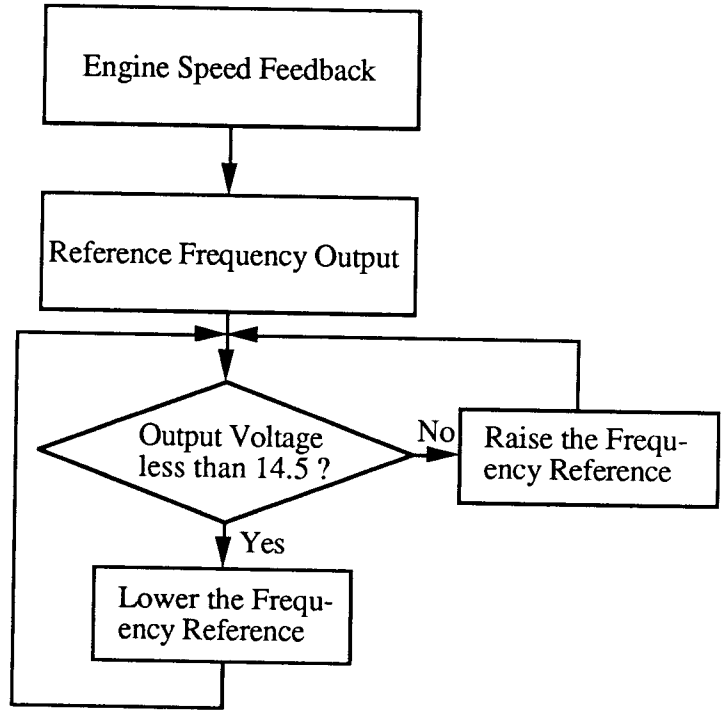

Fig. 4.4 EMU Operation

A simple electronic circuit designed to accomplish this operation is shown in Appendix II. The scheme uses both the speed feedback as well as the output voltage feedback and generates a 'Frequency Control Input' signal for the SPG. In a practical automotive application, the engine speed information can be obtained using the 'timing signals' generated for the electronic fuel injection system. However, this requires additional external wiring into the alternator

casing. A better approach, which avoids this, is suggested in Section 6.2.

In order to illustrate the efficiency maximization principle, the alternator is run at an approximately constant speed, 6100 rev/min. (101 rev/s). The system voltage is maintained at 14.5V and a 25A load is connected (constant electrical output power, 362.5W). The inverter output frequency is varied over a range and the results are shown in Table 4.1.

Table 4.1. Efficiency Maximization Test
(constant electrical output power = 362.5W)

Alt. torque (N-m)	Mech. power (W)	2-pole frequency (Hz)	6-pole frequency (Hz)	2-pole rms line voltage (V)	2-pole rms current (A)	D.C. link current (A)	% Efficiency
2.1	1312.8	55	348	10.5	18.8	11.5	27.6
1.8	1179.6	60	345	11.4	17.2	8.1	30.7
1.6	1042.3	66	338	12.3	14.9	3.4	34.8
1.4	902.3	74	330	13.2	12.8	-1.8	40.2

where, % Efficiency = 100 [Mechanical Power / Electrical Power]

It can be seen that as the 2-pole (inverter output) frequency is increased, the 2-pole current reduces and so does the alternator input torque. Thus, while maintaining constant electrical output power, the mechanical input power decreases and the system efficiency is improved. The best efficiency is obtained at 74Hz, when the 2-pole

winding starts regenerating. This is indicated by the reversal of the d.c. link current, i.e. active power flows from the control winding to the battery through the inverter. Since the minimum excitation current needs to be maintained, the maximum frequency is limited by the 2-pole line voltage available from the d.c. bus.

Fig. 4.5 shows the curve of efficiency Vs. frequency. Fig. 4.6 shows the 'V/F' relationship obtained by plotting the 2-pole line voltage Vs. the 2-pole frequency.

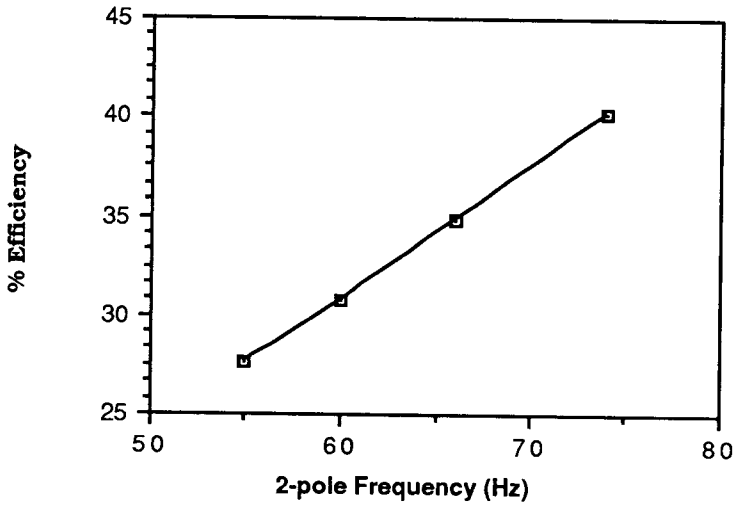

Fig. 4.5 Efficiency Maximization Principle
(for constant electrical output power = 362.5W)

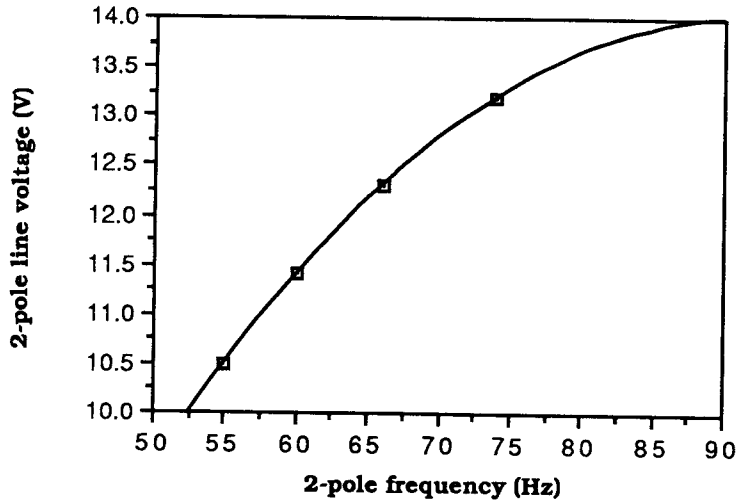

Fig. 4.6 2-pole V/F Relationship

(for constant output power = 362.5W)

Chapter 5.

Test Results for the Brushless Doubly-Fed Automotive Alternator (BDFAA)

The prototype alternator is tested for performance studies using the system configuration as shown in Fig. 1.4. The power winding of the machine feeds the power rectifier. The rectifier in turn charges the battery and supplies the loads. The control winding is supplied through the 3-phase PWM inverter. The VRC maintains the system voltage at 14.5V.

The machine is tested at various load and speed conditions using the same test set-up employed for testing the Lundell alternator (Fig. 1.2). The machine is operated in the synchronous mode with a 'Negative Sequence Excitation.' The results shown, represent the most efficient operating point at any particular load current. This point is achieved by means of frequency variation as described in Section 4.3. Test data and results are shown in Table 5.1. The maximum alternator speed is limited to about 6000 r/min (i.e. 100 r/s) as in the case of a commercial alternator operation. The prototype alternator system can deliver a maximum of 25A load current while maintaining the output voltage at 14.5V. Therefore, the test data up to that point only is presented.

Fig. 5.1 shows the curves of efficiency Vs. alternator speed at various load currents.

Table 5.1. Test Data for the prototype Brushless Doubly-Fed Automotive Alternator

Alt. speed (r/s)	Alt. torque (N-m)	Mech. power (w)	Output voltage (V)	Output current (A)	Elect. power (w)	% Effi-ciency	2-pole line voltage (V) rms	2-pole current (A) rms	2-pole freq. (Hz)	6-pole freq. (Hz)	D.C. link current (A)
31.8	3.1	609.8	14.5	5	72.5	11.9	11.8	13.7	30	100	4.1
51.8	1.0	322.6	14.5	5	72.5	22.5	11.8	9.5	42	167	0.9
67.2	0.7	297.9	14.5	5	72.5	24.3	12.7	7.3	58	217	-1.0
83.0	0.6	303.0	14.5	5	72.5	23.9	12.6	6.1	71	250	-0.8
101.1	0.5	339.9	14.5	5	72.5	21.3	12.6	5.4	87	323	-1.0
49.7	2.1	665.6	14.5	15	217.5	32.7	12.4	14.3	36	156	1.3
66.3	1.3	559.8	14.5	15	217.5	38.9	13	11.1	52	213	-1.2
82.7	1.0	538.2	14.5	15	217.5	40.4	13.1	9.4	66	263	-2.1
101.2	0.9	572.3	14.5	15	217.5	38.0	13.1	8.6	80	313	-2.2
54.1	3.2	1087.2	14.5	20	290.0	26.7	11.4	18.9	34	161	7.5
68.6	1.6	706.3	14.5	20	290.0	41.1	13.1	12.7	52	218	-1.7
84.4	1.3	682.5	14.5	20	290.0	42.5	13.2	11.2	65	268	-2.2
100.6	1.1	712.7	14.5	20	290.0	40.7	13.2	10.5	78	322	-2.5
67.7	2.2	944.4	14.5	25	362.5	38.4	12.8	15.5	48	213	0.1
85.0	1.7	894.5	14.5	25	362.5	40.5	13.2	13.7	62	272	-1.1
101.7	1.4	902.3	14.5	25	362.5	40.2	13.2	12.8	74	328	-1.8

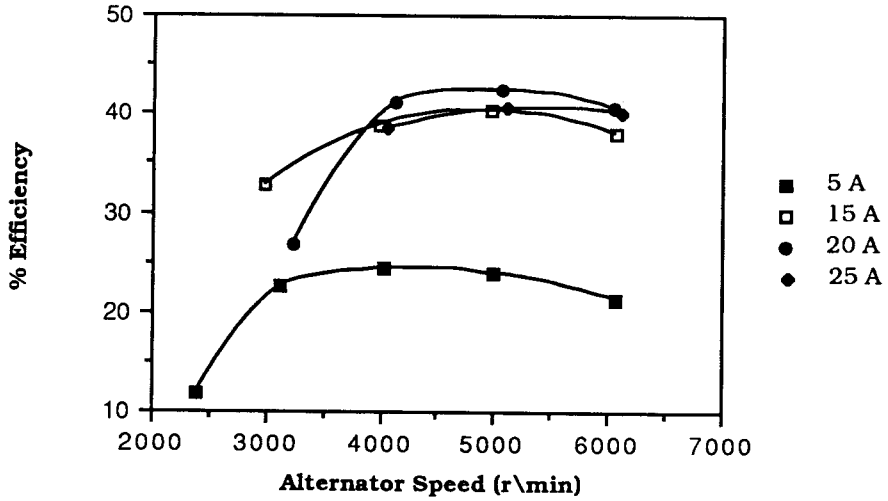

Fig. 5.1 BDFAA Performance

Chapter 6.

Conclusions
and
Recommendations for Future Improvements

6.1 Conclusions

A comparison of Fig. 1.3 and Fig. 5.1 indicates that the proposed alternator system has the potential to compete with the existing car alternator system. Fig. 6.1 shows the performance comparison for 15A load current.

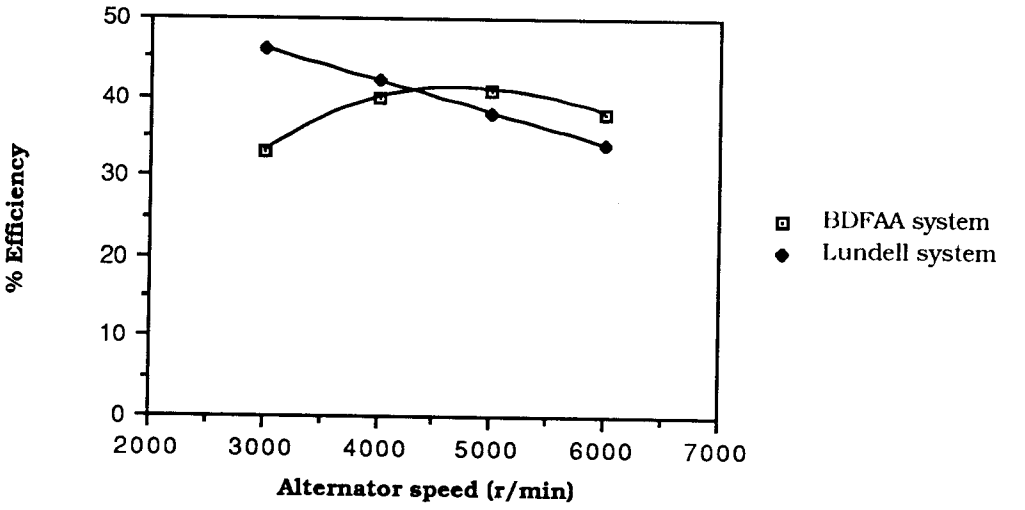

Fig. 6.1 Performance Comparison
(Alternator output current 15A, at 14.5V)

Unlike in the conventional system, the efficiency curves for the BDFAA system do not vary significantly with speed. This fact is very important as it indicates that the proposed system can maintain good performance over a wide speed range. This is essentially achieved by means of the EMU.

Efficiency figures for the prototype BDFAA system are lower than the conventional system figures. However, this is not the case over the entire speed range. The reason for this is the speed for which the machine is optimized. The conventional system seems to be optimized for lower speeds whereas the BDFAA system works better at medium and higher speeds. The speed range can easily be altered by changing the engine-to-alternator pulley ratio as required.

The main reason for low efficiency of the prototype system is the machine size. The prototype machine is wound in an induction machine frame that was readily available. The machine stack is too long for the desired output level, resulting in a large magnetizing requirement, i.e. large control winding currents. In turn, the high control winding currents result in excessive copper losses. Since the inverter supplying the control winding acts as a load on the system, overall efficiency is reduced.

Also, these high currents the inverter as well as rectifier result in higher device losses. Low inverter efficiency also brings down the overall system efficiency.

These problems can be solved by optimizing the machine geometry for the desired output. With that improvement, the machine can be expected to support higher load currents than the prototype machine, which is limited to 25A load current at 14.5V. However, it

has been observed that even the conventional alternator system is not capable of maintaining the output voltage at 14.5V at high load currents.

Other advantages offered by the proposed system are robust and inexpensive structure, brushless operation and no size limitations.

The performance of the two power-electronic units (the rectifier and the inverter) is seen to be very important. A high rectifier efficiency is achieved using Schottky diodes. The inverter efficiency is low because the device drop, though only 1-2V, is a substantial percentage of the 14.5V system rating. Therefore, the use of low voltage drop devices is very important for both the rectifier and inverter.

The performance of the Voltage Regulator Circuit (VRC) is found to be quite satisfactory. The circuit is simple and offers an easy calibration method. The Efficiency Maximizer Unit (EMU) carries out the important task of maintaining maximum efficiency operation over a wide speed and load range. This circuit is also quite simple. It also ensures that the system voltage is maintained at 14.5V by generating appropriate frequency reference signals. A higher precedence is given to the system voltage than to the efficiency maximization, since a low system voltage can adversely affect electrical and electronic loads in the automobile.

One possible limitation of the BDFAA system could be the requirement of an initial excitation source. The machine, being similar to an induction machine, does not have any remnant field. In the case of a conventional system, if the battery is discharged, the remnant field in the rotor can provide self-excitation and can initiate

the voltage build-up (using push-start). This is not possible with the BDFAA system. However, in modern vehicles with automatic gears a push-start is not possible. Also, most vehicles with computerized systems (i.e. fuel injection) will not start for safety reasons if the battery voltage is below a certain level. Therefore, the only way to start the engine is by externally providing the rated voltage, e.g. by means of a jump-start.

6.2 Recommendations for Future Improvements

A smaller machine (i.e. shorter stack) with more copper area needs to be designed. This will improve the regulation and overall efficiency. This will also bring down the device ratings allowing the use of smaller, cheaper or more efficient devices. Different devices like MOSFETs or BJTs (not in Darlington configuration) can be tried for the inverter once the current levels come down.

For the prototype machine, the only configuration tested was one with a 6-pole power winding and a 2-pole control winding. A different pole number configuration needs to be investigated, keeping in mind the capability of power generation through the control winding.

It is brought out in Section 6.1 that the low system voltage (14.5V) is a cause of the inefficient system operation. The automobile manufacturers are already planning to go to higher voltage systems such as 24V, 36V or even 48V. With the higher voltage systems, the current ratings would go down for the same output requirements. This will help in achieving better efficiencies. Hence, it is quite clear that

systems at higher voltages would be much more efficient and need to be developed.

The BDFM can generate with d.c. excitation applied to the control winding. This mode has not been explored fully yet for the prototype BDFAA. Though efficiency maximization is not possible with d.c. excitation, under certain conditions, this mode may offer some advantages with a properly designed machine. For example, even if the battery is almost discharged, a relatively higher d.c. excitation current can be supplied for a short duration to initiate the generation. The a.c. excitation current in this low voltage situation would be limited by the inductive reactance of the control winding.

The inverter circuit can be adapted to provide d.c. excitation by turning on any two upper devices and one lower device in the remaining leg, or vice versa. A d.c. modulating signal instead of sinusoidal modulating waves will allow chopper control to regulate the output voltage.

As mentioned in Section 6.1, the machine seems to work better at higher speeds. Therefore a high pulley ratio can be used to run the machine at higher speeds, even when the engine is idling. Another option is to design a machine for lower speed operation.

The EMU uses engine speed feedback. In the case of the prototype alternator system, it has been observed that the efficiency is optimized for minimum d.c. link current flowing into the inverter, or, during regeneration, for maximum d.c. link current flowing out of the inverter. Thus, a current feedback from the d.c. link can also be used to develop the efficiency maximization unit. This would eliminate the

need of external wiring into the alternator casing, since the inverter and the alternator would be in the same enclosure.

The prototype alternator does not provide any system protection. Current and voltage limiters are required in the inverter as well as rectifier circuits to prevent damage.

Finally, system integration is an important task to be considered. The entire semiconductor portion can be put in a single package using SmartPower technology. For the first level of integration, the rectifier and inverter can be replaced separately with units available in compact packages. An integrated system would also improve efficiency, since losses and voltage drops in leads would be minimized.

BIBLIOGRAPHY

[1] Nady Boules, "Performance Requirements for Future Automotive Electrical Machines", Proceedings: NSF Workshop on Electrical Machines and Drives, 1988. pp 16-21.

[2] R. Wang, N.A. Demerdash, "Extra High Speed Modified Lundell Parameters and Open/Short Circuit Characteristics from Global 3D-FE Magnetic Field Solutions", IEEE PES Winter Meeting, New York, 1991. Paper 91WM067-9EC.

[3] L.M.C. Mhango, "An Experimental Study of Alternator Performance Using Two Drive Ratios and a Novel Method of Speed Boundary Operation", IEEE IAS Annual Meeting, Seattle, 1990. pp 301-308.

[4] R.D. King, "Combined Electric Starter and Alternator System Using a Permanent Magnet Synchronous Machine", U.S. Patent No. 4,862,009.

[5] A.K. Wallace, R. Spée, "Brushless Doubly-Fed Generation System for Vehicles", US Patent No. 07/560,188.

[6] V.Javadekar, Ravi D.K., R. Spée, A. Wallace, " A Variable-Speed Brushless Doubly-Fed Automotive Alternator", Conf. Rec., EPE,Florence,1991.pp 4-099 - 4-103.

[7] L.J. Hunt, "A New Type of Induction Motor", IEE Journal, 1921. Vol.59, pp 648-677.

[8] F. Creedy, "Some Developments in Multi-Speed Cascade Induction Motors", IEE Journal,1921. Vol.59, pp 511-521.

[9] A.R.W. Broadway, B.J. Cook, P.W. Neal, "Brushless Cascade Alternator", IEE Proc. 1974, Vol.121, pp 1529-1535.

[10] H.K. Lauw, "Characteristics and Analysis of the Brushless Doubly-Fed Machine", Final Report, US DOE, Contract No. 79-85BP24332, 1989.

[11] R. Spée, A.K. Wallace, H.K. Lauw, "Simulation of Brushless Doubly-Fed Adjustable Speed Drives", Conf. Rec. IEEE IAS Annual Meeting,San Diego,1989. pp 738-743.

[12] Ned Mohan, T.M. Undeland, W.P. Robbins, 'Power Electronics: Converters, Applications and Design'. Wiley,1989.

[13] S.R. Bowes, A. Midoun, "Suboptimal Switching Strategies for Microprocessor-Controlled PWM Inverter Drives", IEE Proc. Vol.132, Pt.B,No.3,May 1985. pp 133-148.

[14] P.N. Enjeti, P.D. Ziogas, J.F. Lindsay, M.H. Rashid, "A New PWM Speed Control System for High-Performance ac Motor Drives",

IEEE Trans. Ind. Electronics,Vol.37,No.2, Apr.1990. pp 143-151.

[15] B.K.Bose, ' Power electronics and AC drives', Prentice-Hall, NJ, 1989.

[16] J.T. Boys, P.G. Handley, "Harmonic Analysis of Space Vector Modulated PWM Waveforms", IEE Proc. Vol.137,Pt.B, No.4,July 1990. pp 197-204.

[17] V.P. Ramamurthi, B. Ramaswami, "A Novel Three-Phase Reference Sine-Wave Generator for PWM Inverters", IEEE Trans. Ind. Electronics, Vol.IE-29,No.3,Aug.1982. pp 235-240.

[18] P. Rochelle, R. Spée, A.K. Wallace, "The Effect of Stator Winding Configuration on the Performance of BDFM in Adjustable Speed Drives" Conf. Rec. International Conference for Electrical Machines, Cambridge, Mass., 1990. pp 54-59.

[19] Ken Layne, 'Automobile Electronics and Basic Electrical Systems', Wiley, 1990.

[20] Robert G. Irvine, 'Operational Amplifier Characteristics and Applications', Prentice Hall, 1987.

[21] Benjamin C. Kuo, 'Automatic Control Systems', Prentice Hall of India Pvt. Ltd., 1985.

APPENDICES

APPENDIX I

Technical Data for Power Transistors

Technical Data for Power Diodes

Technical Data for Power Transistors
(from Motorola Bipolar Power Transistor Data-book)

MJ11011 PNP
MJ11012 NPN
Darlington Power Transistors
Complementary Silicon

Maximum Ratings

Collector-Emitter Voltage	:	V_{CEO}	:	60Vdc
Collector-Base Voltage	:	V_{CB}	:	60Vdc
Emitter-Base Voltage	:	V_{EB}	:	5Vdc
Collector Current	:	I_C	:	30Adc
Base Current	:	I_B	:	1Adc

Electrical Characteristics

DC Current Gain	:	h_{FE}	:	1000 min. @ I_C = 20 Adc, V_{CE} = 5 Vdc.
Collector-Emitter Saturation Voltage	:	$V_{CE(sat)}$	:	3 Vdc max. @ I_C = 20 Adc, I_B = 200 mAdc.
Base-Emitter Saturation Voltage	:	$V_{BE(sat)}$	:	3.5 Vdc max. @ I_C = 20 Adc, I_B = 200 mAdc.

Technical Data for Power Diodes
(from Motorola Rectifiers Data-book)

1N1184A
Medium Current Rectifier

Maximum Ratings

Peak Repetitive Reverse Voltage	:	V_{RRM}	:	100 V
Average Rectified Forward Current	:	I_O	:	40 A
Peak One-Cycle Surge Current	:	I_{FSM}	:	800 A

Electrical Characteristics

Maximum Forward Voltage @ 100A	:	V_F	:	1.1 V

1N5834
Schottky Barrier Rectifier

Maximum Ratings

Peak Repetitive Reverse Voltage	:	V_{RRM}	:	40 V
Average Rectified Forward Current	:	I_O	:	40 A
Peak One-Cycle Surge Current	:	I_{FSM}	:	800 A

Electrical Characteristics

Maximum Forward Voltage @ 40A	:	V_F	:	0.590 V

APPENDIX II

Circuit Diagrams

Switching Pattern Generator (SPG)

Voltage Regulator Circuit (VRC)

Efficiency Maximization Unit (EMU)

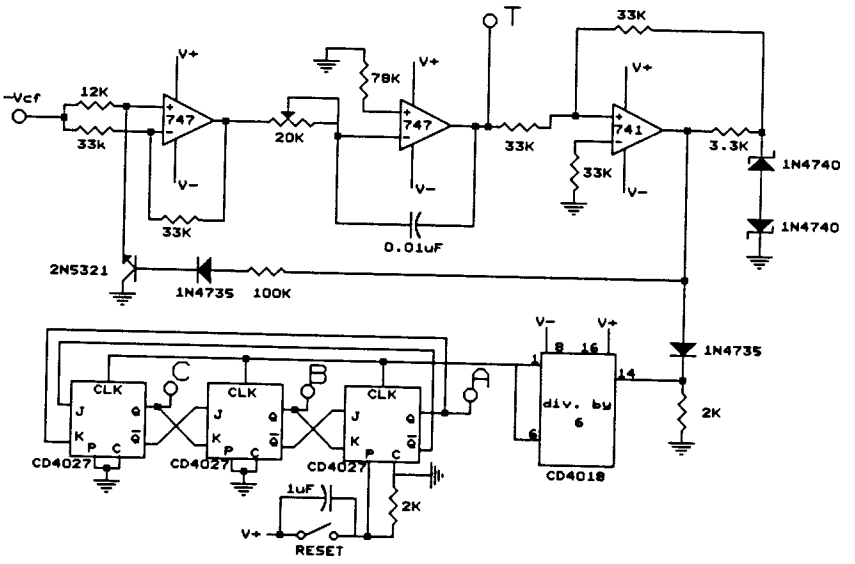

CARRIER WAVE AND THREE PHASE SQUARE-WAVE GENERATOR

Fig. II.1 SPG - Carrier Wave and Three Phase Square Wave Generator

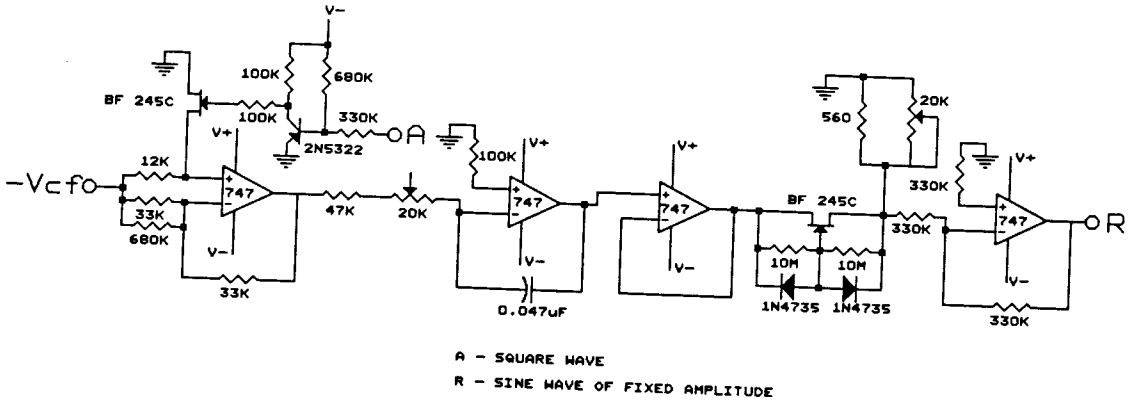

SQUARE WAVE TO SINE WAVE CONVERTER
(ONE FOR EACH PHASE - A,B,C)

Fig II.2 SPG - Square Wave to Sine Wave Converter

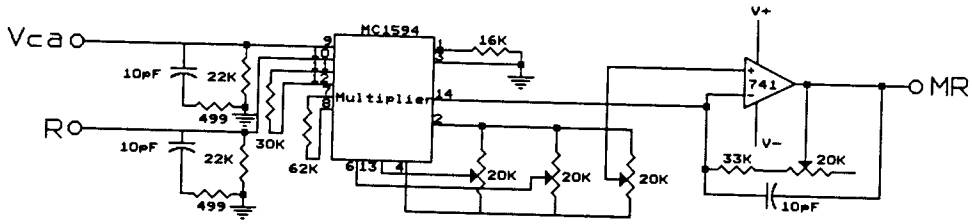

Vca - VOLTAGE CONTROL REFERENCE
R - SINE WAVE OF FIXED AMPLITUDE
MR - MODULATING SINE WAVE OF VARIABLE AMPLITUDE

MULTIPLIER
(ONE FOR EACH PHASE - R, Y, B)

Fig II.3 SPG - Multiplier

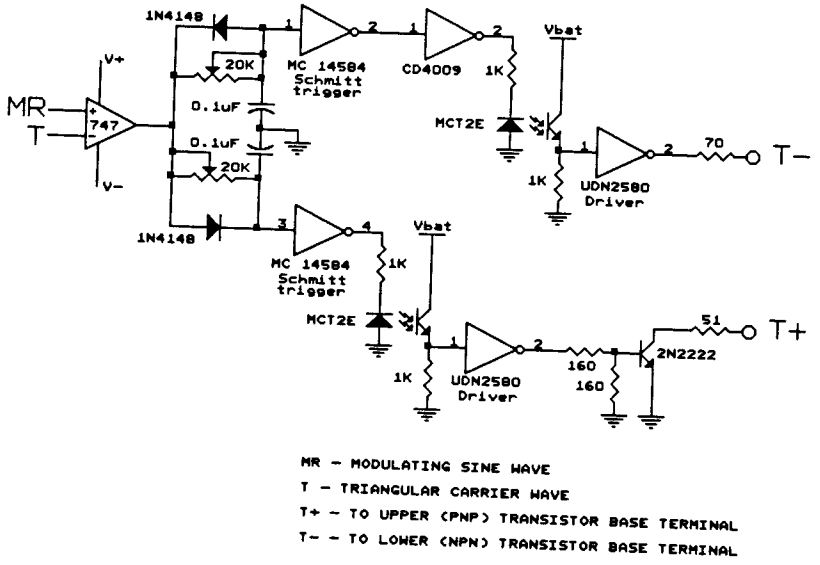

COMPARATOR, BLANKING TIME ADDER,
OPTO-ISOLATOR AND DRIVER CIRCUITRY
(ONE FOR EACH PHASE - MR, MY, MB)

Fig II.4 SPG - Comparator, Blanking Time Adder, Opto-Isolator and Driver Circuitry

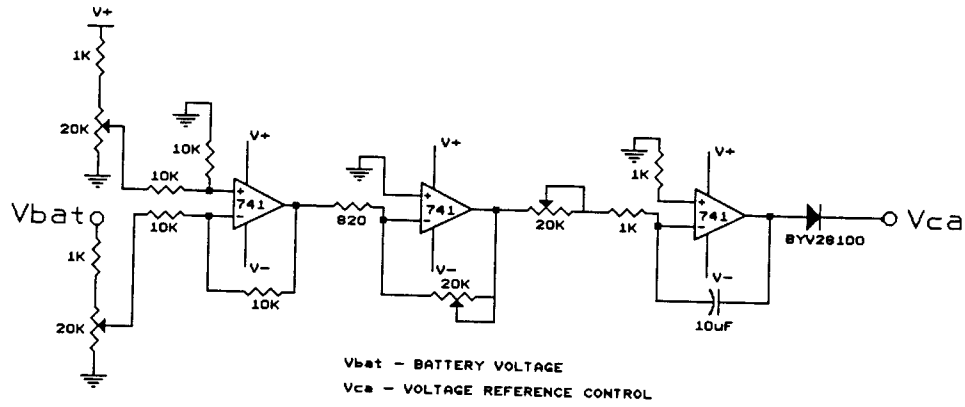

Fig. II.5 Voltage Regulator Circuit (VRC)

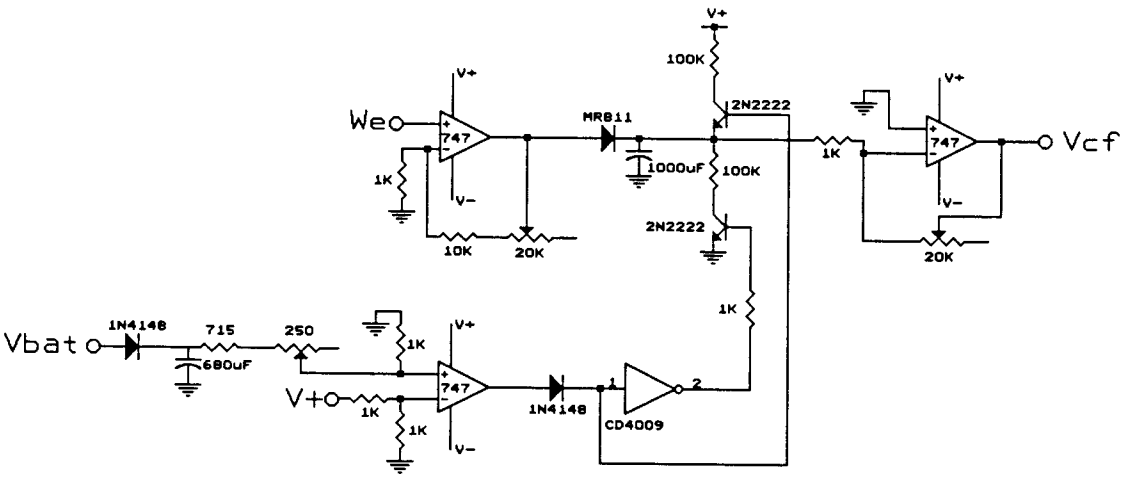

We - ENGINE SPEED SIGNAL
Vbat - BATTERY VOLTAGE
Vcf - FREQUENCY REFERENCE CONTROL

Fig. II.6 Efficiency Maximization Unit (EMU)